Multiphase flow in large diameter pipes

by

Garaev Damir MSc

Thesis submitted as part of the requirements for the Degree of Master of Science (by Research)

In

Petroleum and Environmental Engineering

University of Nottingham

School of Chemical and Environmental Engineering

September 2011

Multiphase flow in large diameter pipes

To my big family…

Abstract

Knowledge of multiphase flow is essential for many industries and the vast majority of work on this topic has been done using pipes of 25-50 mm. However, developments in a number of industries, from heat exchangers to large diameter deep water risers need the knowledge to use larger diameter pipes, in which the behavior of multiphase flow may be different from that in smaller diameter pipes.

In the present study the experiments in vertical air/water two phase upflow were performed using a riser of 127 mm in diameter at different pressure to change the density of the gas. Data on void fraction were gained using a Wire Mesh Sensor (WMS). The data were analyzed to obtain flow patterns, frequency etc. Using these data comparison with different prediction methods was carried out.

Table of contents

Acknowledgements

It would not have been possible to write this thesis without the help of many kind people around me, only few of them it is possible to mention here.

Above all, I am sincerely and heartily grateful to my respected supervisor Professor Barry J. Azzopardi. His support, encouragement, patience and enthusiasm from the very beginning to the end of the course enabled me with the understanding of the subject and developed many of my skills so much.

I am truly thankful to PHD students of the Department Mukhtar Abdulcadir, Abolore Abdullah, Safa Sharaf, Peter Van der Mullen who readily shared their knowledge with me.

I would like to thank the laboratory technicians, especially chief engineer Phil Bennett and Paul Bramman for their help and brilliant ideas during maintenance and improving of the rig.

Without my coursemates Rustam Akhmetov, Radjap Omar, Yaseen Taha the time in The UK would not be so great. I am really grateful to them for the continuous help during the course.

I owe sincere and earnest thankfulness to my wife Asel for her personal support and great patience at all times. I am indebted to my sister, grandmother, step father who have contributed a lot to my work by extensive encouragement.

Words can not express my gratitude to my mother whose support, patience and help made my study in the UK possible.

Lastly, I offer my regards to all of those who supported me in any respect during the completion of the thesis.

Nottingham, September 2011.

List of tables and figures

Chapter 1

Introduction to multiphase flow

The flow of fluids can be encountered in many areas of engineering and technology. Majority of flows in power generation, oil/gas production, chemical industries consist of more than one phase. This type of flow is called multiphase flow. The word multi means "more or many" and is the contrary of "single" which means one. Multiphase flow is widely found in different types of equipment like chemical reactors, phase separators, heat exchangers, and pipelines. A deep and thorough understanding of multiphase flow is crucially important for equipment design, minimizing of capital costs, efficacious and safe operation. There are many possible combinations of multiphase flow: gas/liquid, solid/liquid, solid/gas, two or more immiscible liquids (oil/water) and sometimes more than two phases (liquid/oil/gas). Azzopardi (2006)

Some examples will be given to illustrate possible applications. In hydrocarbon production oil, gas, water, sand are moved to the surface through a well. Multiphase flow happens as vapour/liquid flow in power generation equipment, in this case with high chances for phase change. In case of depletion of a reservoir the amount of water (water cut) in the multiphase flow will go up, consequently the efficiency of the process must go up, desirably without increasing of the costs and investments – to acquire as much hydrocarbons as possible from the mixture.

Analysis of recent published papers shows that multiphase flow in larger diameter pipes is of increasing interest. This may be result of the growth in offshore gas and oil production, as transportation in that case needs relatively long pipes of large diameter to minimize pressure drop (Omebere-Iyari 2007, 2008). According to Yoneda et al. (2002) the use of large diameter pipes can significantly improve performance of the equipment in nuclear industry.

It was noticed that although multiphase flow in large diameter pipes is very important and many papers have been recently published on this area, much more available papers are devoted to smaller diameter pipes (Omebere-Iyari 2008). Thus exploring this area is serious and perspective field of study.

Since there is lack of data on multiphase flow in larger diameter pipes this thesis focuses on obtaining experimental results in 127 mm wide vertical riser. Research was carried out to investigate void fraction characteristics at 0, 1, and 2 bars pressure to study the effect of pressure.

1.1 Gas/liquid flow

Research in the field of multiphase flow is crucial for many aspects of engineering. There are common types of multiphase flow as gas/solid, liquid/liquid, gas/liquid/solid, and liquid/solid. Hydrocarbons obtained from oil and gas fields always consist of natural gas and oil or condensed hydrocarbons with higher molecular weights than the gas. This multiphase mixture is lifted from the ground to the surface through the piping of the well. Modern well technologies allow the tapping of hydrocarbon reservoirs miles away from the production site, the tubing may be at a wide range of orientations from vertical to horizontal. The same applies for pressure drop, flow rate, pipe diameter. There is a demand for knowledge on mixture behavior inside the pipes to inform engineers working on corrosion inhibitor techniques. At the platform or ground level usually a choke valve is to control the flow. Then, the flow is sent to the processing area trough bends, expansions, and different fittings until it comes to the main separator where the phases are separated and pumped to the refinery or shore terminal. Under certain conditions it can be more reasonable from economical point of view to move the flow as a multiphase mixture over land or seabed. For these reasons understanding of the conditions at which the mixture arrives is most important as is the combination of the phases at combining and dividing pipes. (Azzopardi 2006)

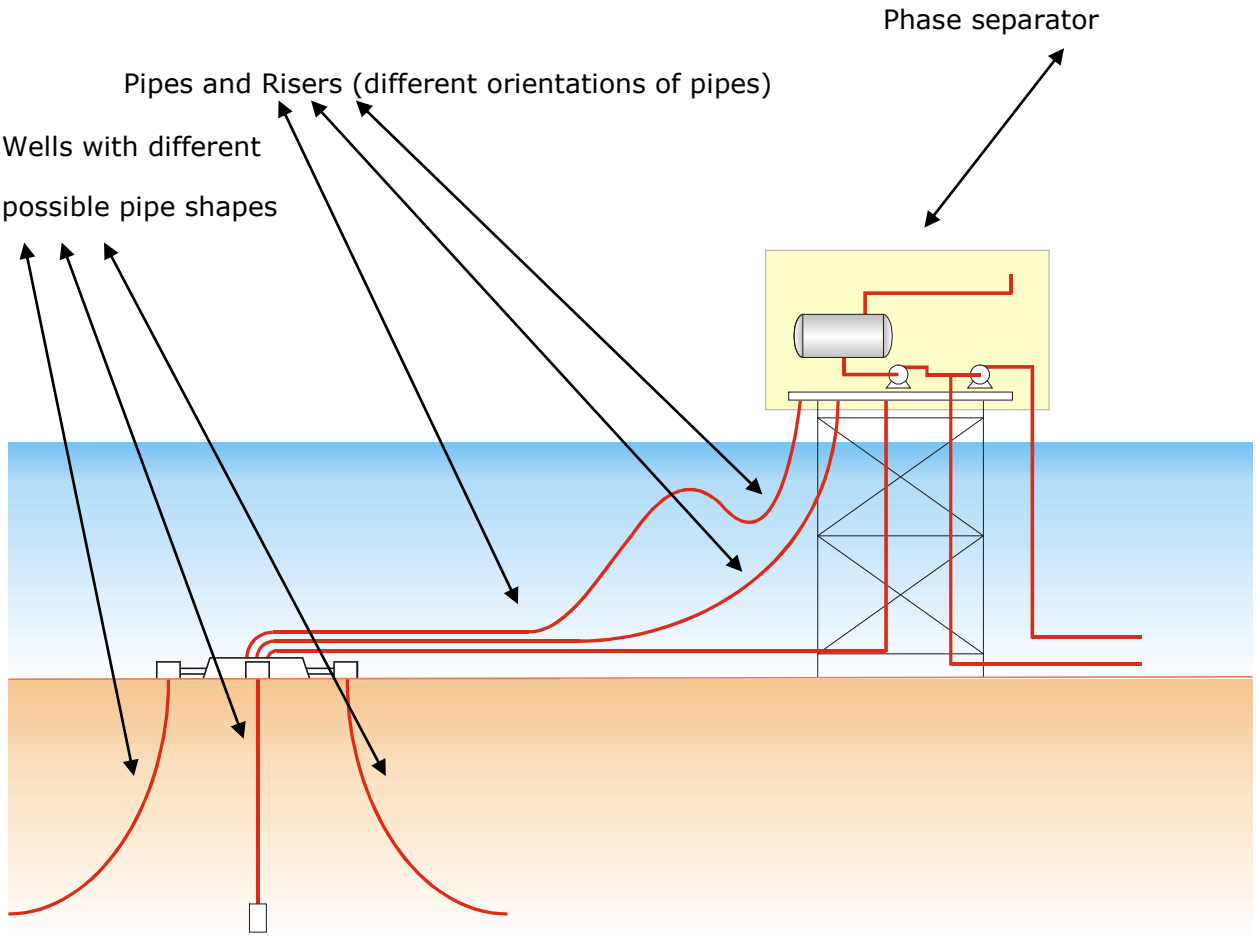

Figure 1.1 Schematic of an offshore oil/gas production facility. (Azzopardi 2006)

In the refining and chemical process industries majority of product separations need distillation columns all of them require a supply of vapour at the bottom and liquid at the top. These are provided by heat exchangers, for vapour they are called – reboilers, for liquid – condensers. These heat exchangers are very big energy consumers; therefore accurate design is especially essential. Multiphase flow occurs not only inside these units, but also in the pipes connecting them to the distillation column. In the power generation industry where the generation of vapour is the main task boilers and condensers are also used. Therefore multiphase flow is extremely important in wide range of engineering areas and for understanding of multiphase flow knowledge of the fundamentals of other subjects like fluid dynamics and thermodynamics is important.

1.2 Gas-liquid flow patterns

Photography of multiphase flow is useful technique to obtain understanding the different flow regimes which happen with changing phase parameters such as pressure, velocity, density. From such experiments data can be presented as graphs which become flow pattern maps. Figure 1.2 illustrates the range of flow patterns in vertical pipes. Flow patterns in horizontal pipes are considered later in this chapter.

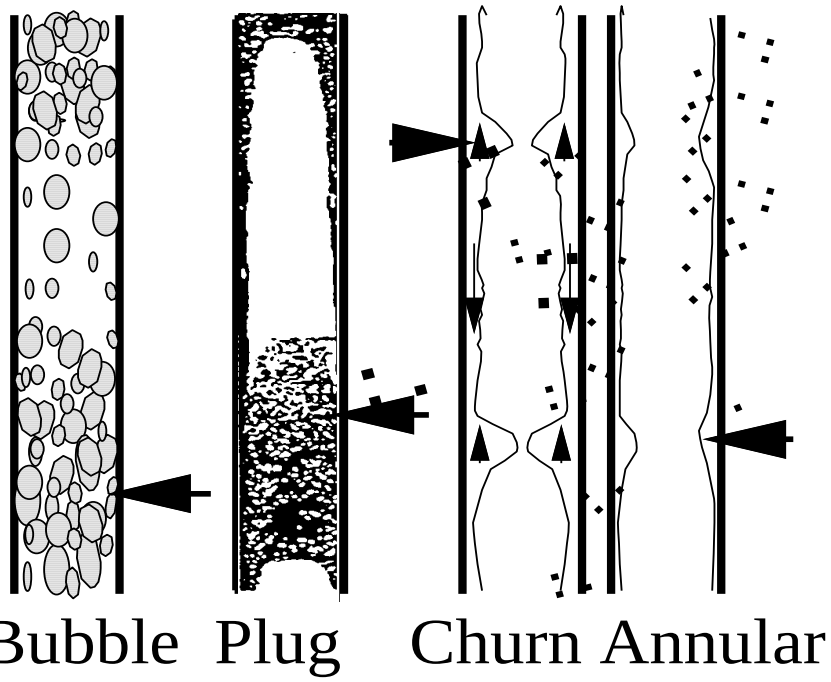

Figure 1.2 Vertical flow patterns for gas/liquid flow (Azzopardi and Hills 2001)

1.3 Vertical gas liquid flow

Figure 1.2 (Azzopardi and Hills 2001) shows the characteristics of gas-liquid vertical upflow, the authors identify four main flow patterns

- Bubbly flow

In this case there is gas phase scattered as bubbles within continuous liquid phase. The bubbles move with complex motion inside the flow, may be uniting and usually are of uniform size. Sometimes they gather in the tube centre, Serizawa and Kataoka, 1988 named this as wall-peaking and core-peaking flows, which can be considered as sub-patterns of bubbly flow. At lower liquid velocities, the small bubbles are formed at the gas distributor or

in the process of nucleate boiling, while at higher liquid velocities they may occur because of turbulent breakage of larger bubbles. These two sub-categories can be called discrete bubbly or dispersed bubbly flow. The concentration of bubbles is not constant but there are waves of concentration which move along the pipe.

- Plug flow

This flow regime which in vertical risers is called slug flow, happens when coalescence starts and the bubble size tends to the direction of the channel. The bullet shaped bubbles which often are referred as Taylor bubbles travel up the tube surrounded by a thin film of liquid. The liquid between the bubbles usually has a dispersion of smaller bubbles within it. Cheng et al 1998 have found that this pattern does not occur in large diameter pipes (150 mm) and the flow changes from bubble to churn flow.

- Churn flow

At relatively high velocities the Taylor bubbles in slug flow break down and become unsteady pattern in which a churning or oscillatory movement of liquid in the pipe occurs. Churn flow covers a wide range of gas flow rates and is an important pattern. At the lower velocities, it may be regarded as shattering plug flow with occasional bridges of liquid across the pipe, sometimes this flow is called semi-annular flow; at higher gas velocities it can be considered as degenerate type of annular flow with the direction of the film flow changing and very big waves appearing on the interface. Churn and plug flow patterns demonstrate high instability in pressure drop, void fraction are often grouped together as intermittent flow.

- Annular flow

In this case flow is characterized as by liquid moving as a film on tube walls. Some of the liquid can be in the form of drops in the middle of the tube. Under certain conditions most of the liquid travels as drops, this kind of flow is mist flow. However only in case of heat transfer systems where walls may become too hot for the liquid to form film mist flow can occur. Interchange of liquid occurs between the droplets and the film. Sometimes bubbles of gas can be formed inside the liquid film. In case of very high liquid flow rates there is so much liquid in the gas core that "wisps" instead of drops appear, this is wispy annular flow.

The identification of flow patterns is of high importance because as the long range of physical processes that they include makes it not likely that a single model may exactly

depict the flow. Flow patterns are important for different aspects. For example, bubble flow creates a big interfacial area and thus is most proper for processes when mass transfer is needed. Therefore bubble columns are applied for reaction and absorption. The interminent flow regimes (plug and slug flow) can make vibration damage especially at bends and fittings as the momentum of the gas and liquid dominated areas may be very much different, also these flows are important when two phases need to be separated, because slug flow may make separators designed to work with time averaged gas liquid flow rates fail, if the feed becomes only liquid for periods.

1.4 Flow Pattern Maps for Vertical Upflow

Flow pattern is often presented on a two dimensional diagram in terms of system variables. The most general variables are the gas and liquid superficial velocities (volumetric flow rate/cross sectional area of the tube). As variables other than the superficial velocities can affect the flow pattern, such maps are specific to special combination of geometry and fluids. However there has not been produced any universal flow map.

The usual way of making a flow map is to identify the flow pattern ay certain conditions covering the field, then draw boundary lines separating the different patterns. Because it is difficult to precisely identify flow patterns, it often occur that a few experimental points are on the wrong side of the lines and the lines should be taken as transition zones of indefinite width.

Figure 1.3 demonstrates a recent map for water/air in 82.6 mm tube Zhang et al (1997). On this map boundary lines are based on different objective criteria, not the sketching process. The map is in agreement with semi-theoretical map of Taitel et al (1980) in figure 1.4

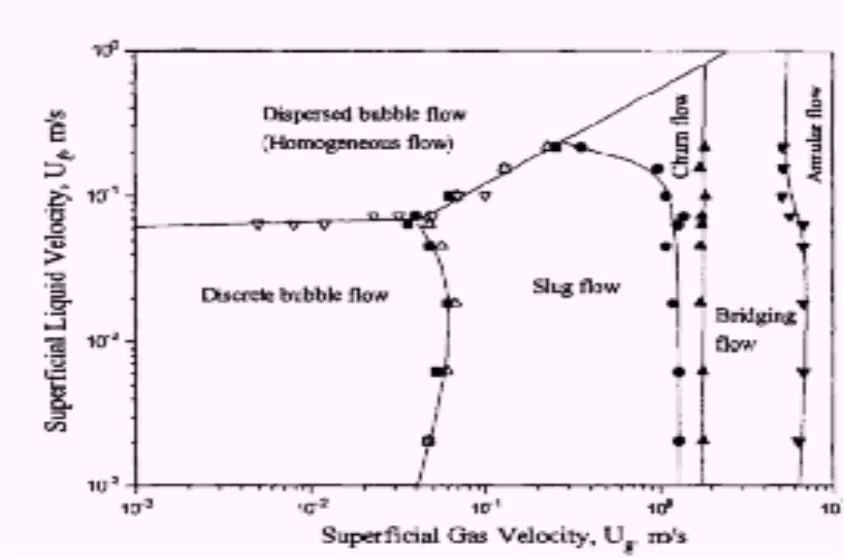

Figure 1.3. Flow pattern map for water/air in 82.6 mm tube Zhang et al (1997).

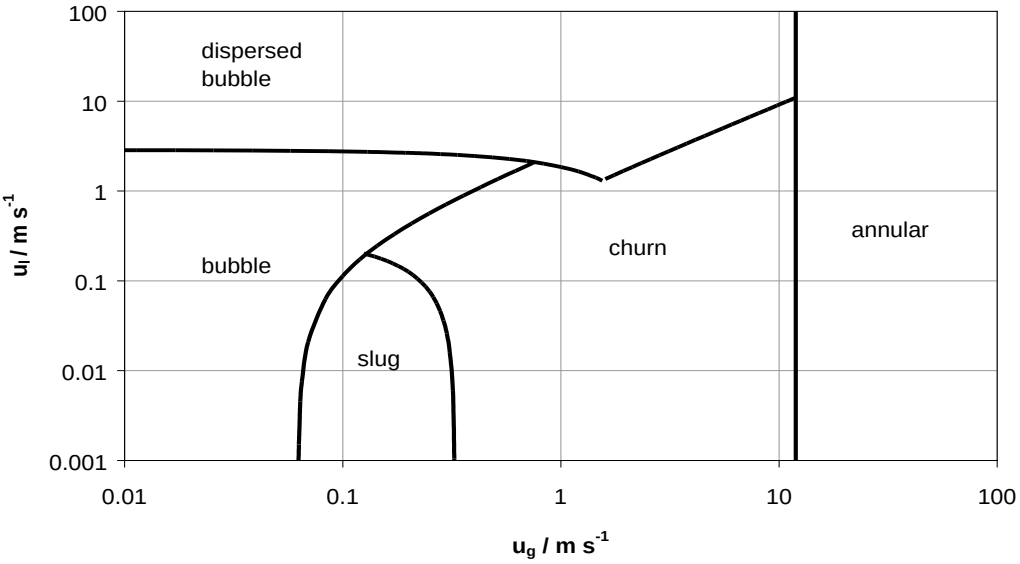

Figure 1.4. Vertical flow pattern map of Taitel et al. (1980)

Other authors have reported maps where the superficial velocities are modified by factors in the form of ratios of physical parameters to standard characteristics raised to different powers. A widespread method which tries to unite some physical reality is that of Hewitt and Roberts (1969) in figure 1.5. The data plotted as $\rho_g u^2_{gs}$ against $\rho_l u^2_{ls}$ (gas momentum flux against liquid momentum flux), and data for water/air at 3 bar and water/steam at 35 and 70 bar were plotted together by this approach.

Figure 1.5. Flow pattern map of Hewitt and Roberts (1969) - vertical upward flow.

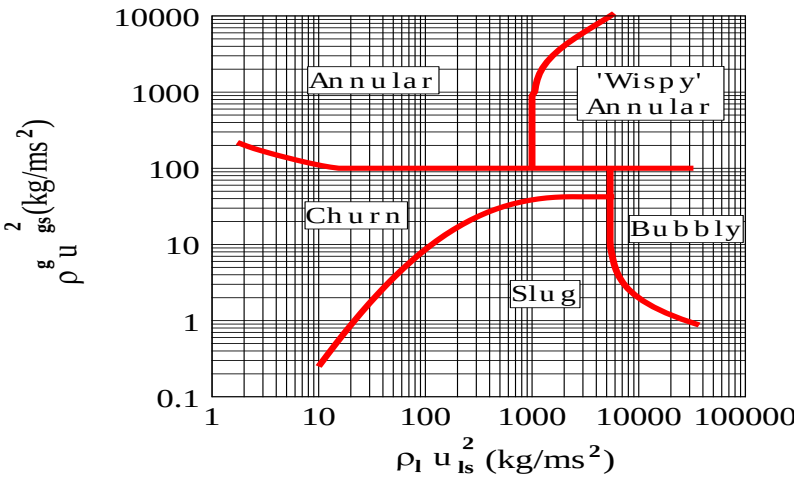

1.5 Flow Pattern transition Models

1.5.1 Transition Involving Bubbly Flow

Many of sub-regimes of bubbly flow have been described, some of them are referred as transition regions between the bubble and slug pattern, for example "cap bubble" and "bubble cluster" of Cheng et al (1998), "coalesced bubble" pattern of Zhang et al (1997), and also "churn – turbulent" regime of Zuber and Findlay (1965). All of the entail appearance of considerably bigger bubbles than in the normal bubbly flow, sometimes it is not clear when the bubble–to–slug transition has happened. Hills (1976) found big bubbles, or areas of high voidage, at high gas velocity in 150 mm riser, he called this pattern slug flow in spite the fact that the Taylor bubbles of classical slug flow in narrower pipes were not present subsequently Hills with colleges classified this pattern as churn flow, whilst Ohnuki and Akimoto (2000) found churn-froth, churn-slug, churn bubbly flow patterns in 200 mm

riser, under circumstances when usual slug flow would be predicted, slug flow was not found in those large diameter pipes.

The size of bubble is a parameter which significance has only recently been realized. In bubbly flow two contrary processes occur: bubble breakage as a result of turbulence in the liquid and bubble coalition as a result of collisions between bubbles. At low liquid velocities turbulence is not big, coalition dominates and equilibrium bubble size big, these big bubbles have twisted, continuously changing forms and go up in spiral or zigzag motion, which encourage coalescence. At higher liquid velocities turbulence goes up, and the equilibrium bubble size is smaller, these smaller bubbles generally spherical, go up rectilinearly, lowering collision. All of this results in the two sub-regimes: discrete bubbly and dispersed bubbly flow patterns.

1.5.2 Discrete bubble to slug transition

In case of discrete bubbly flow, turbulence forces are scanty to shatter big bubbles, if big bubbles are at the beginning of the flow slug flow is likely to appear. In small tubes (smaller than 50 mm for water/air) the Taylor bubbles of slug flow have a lower velocity than smaller bubbles, so the smaller bubbles will tend to unite with Taylor bubbles. This fact was reported by Taitel et al (1980). A likely deduction for this type of pipes is that bubbly flow can become slug flow as the gas velocity goes up, this slug flow, however, can never break down into bubbly flow.

It is evident that entrance conditions especially initial bubble size is most important in the study of this transition. Bubbles produced from porous sinters or perforated holes as well as those generated by nucleate boiling on the surface of the pipe tend to be small and thus lead from the beginning to discrete bubbly flow. Because turbulent breakage is not significant to transition to slug flow will be determined principally by the process of bubble coalescence.

Since non-spherical bubbles have chaotic paths they should collide and unite, hence it may be argued that if tubes are long enough, coalition will always result in slug flow, so that discrete bubbly flow an unsteady entrance effect. It is not easy to test this hypothesis in ambient pressure studies, because the decline in hydrostatic pressure along the pipe causes an expansion of the bubbles and high probability of coalition for that reason.

Radovich and Moissis (1962) modeled coalition assuming that bubbles organize themselves in a cubic lattice and move chaotically with respect to other bubbles in the lattice with a mean fluctuating velocity. The authors described a bubble coalition frequency:

$$f_{BC} = \frac{\bar{c}}{D_t\left[\left(\frac{0.74}{\varepsilon_g}\right)^{1/3} - 1\right]^5} \quad (1.1)$$ The dimensionless frequency $f_{BC}D_t/c$ is illustrated in figure 1.6 as a function of the void fraction, ε_g.

Figure 1.6 Variation of bubble collision frequency with void fraction (Radovich and Moissis 1962)

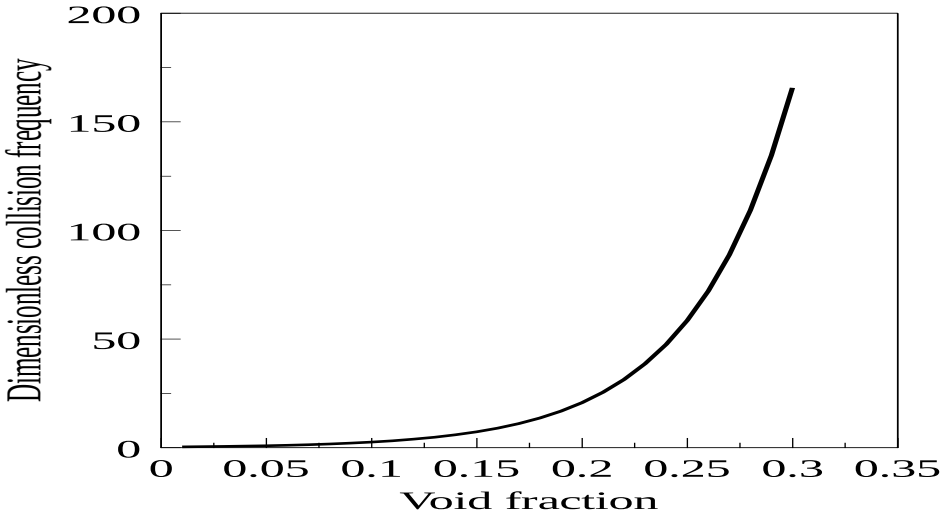

1.5.3 Dispersed bubble to slug transition

Here, the liquid phase turbulence is enough to shatter larger bubbles and it is possible to theoretically find the maximum stable bubble size in any flow. Sevik and Park (1973) considered the bubble breakage by turbulence in continuous phase. The theory leads to a critical Weber number for bubble breakage.

$$We_{crit} = \frac{\rho_l \overline{v^2} r_B}{\sigma} \quad (1.2)$$ here r_B is the radius of bubble, v^2 is the spatial average value of the square of the velocity difference for distance r_B. Sevik and Park (1973) decided that

breakage would happen when resonant frequency of the bubble was identical to a characteristic turbulent frequency. This resulted in good agreement with experiment.

1.6 Transitions at higher gas velocity

Before describing plug/churn and churn/annular transitions it is appropriate to consider flooding and flow reversal which are in use for many of the models of the these transitions. Flooding happens in counter-current flow if the flow rates are so large that one of the phases (usually liquid in gas/liquid flow) cannot continue its flow and is forced back out of the equipment by the other phase. It occurs in different industrial equipment like packed absorption and distillation columns.

In two phase flow in pipes the phenomena is called counter-current flow limitation. It is shown in figure 1.7. Liquid is directed part-way down a vertical pipe through a porous area or is formed in the pipe by condensation. When upflow of gas phase is low the film moves down with small ripples on the interface (a). If gas velocity goes up the size of the ripples increase and their velocity declines, but they stay incoherent.

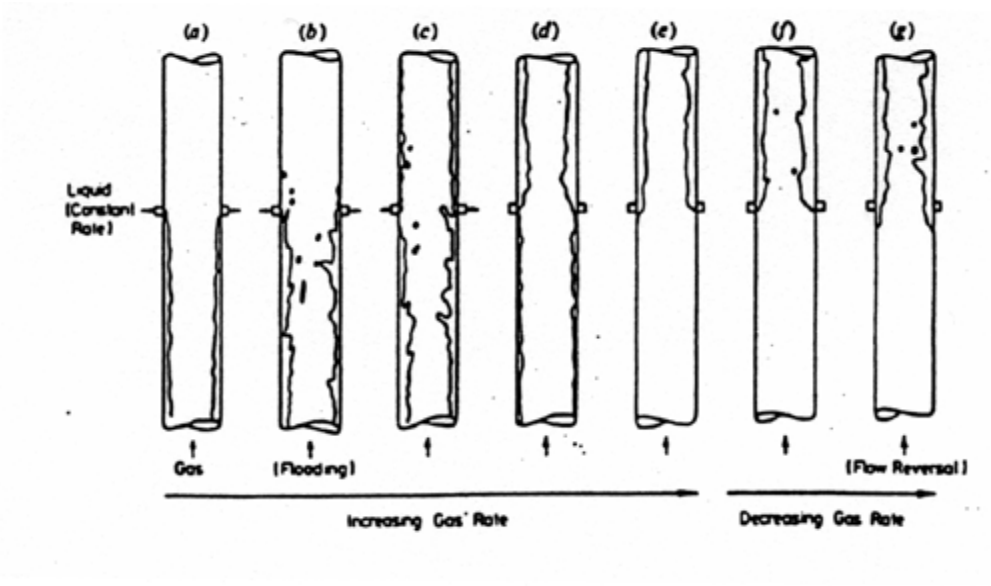

Figure 1.7 Counter-current flow limitation Azzopardi (2006)

Additional increase in gas velocity may suddenly form coherent ring waves at the liquid outlet, which are moved up repeatedly and periodically higher than the liquid inlet , where they form a churn flow (b). This is called the flooding point and there is also a considerable increase and fluctuations in pressure drop. If gas flow rate is further increased moves more liquid up above the liquid inlet, till all the liquid is going up (c). If gas flow is lowered at this point liquid starts to fall below the inlet at the point of flow reversal (d). Further decline of the gas flow rate at the end restores the pure counter – current flow, at the point called deflooding. At all except lowest liquid flow rate there is a hysteresis effect with deflooding occurring at lower gas rates than flooding. The description is theses processes is a compound of papers by Vijayan et al. (2001), Watson and Hewitt (1998), Govan *et al*. (1991). This description refers to small diameter pipes, the three listed papers applied pipes of 25, 26, 31 mm, in which the liquid outlet is a porous sinter, with enough empty pipe beneath to make a fully developed gas flow, and the instability is owe to a big wave being moved up the pipe. Instability begins at the bottom of the pipe, where the waves are biggest.

In larger diameter tubes a different process seems to be, Instead of the big waves appearing at the liquid outlet and being carried up past the pipe inlet, they ascend a small distance before breaking down into high concentration of drops, which is removed in the gas stream and re-deposited higher up in the pipe, increasing the liquid flow rate until it is unsteady in turn. The flow is a churn-kind flow which gradually goes up the pipe further the liquid inlet. Flooding with significant dramatic increase in pressure drop, happens if the churn-kind flow reaches the liquid inlet. This is result of Watson and Hewitt (1998), Vijayan et al. (2001), Zabaras and Dukler (1988), (82 mm, 67 mm, 99 mm respectively).

Wallis (1961) described flooding prediction:

$\sqrt{u_g^*} + \sqrt{u_l^*} = c$ (1.3) where u_g^* and u_l^* are dimensionless superficial velocities:

$$u_g^* = \frac{u_{gs}\sqrt{\rho_g}}{(g D_t \Delta\rho)^{1/2}}; \qquad u_l^* = \frac{u_{ls}\sqrt{\rho_l}}{(g D_t \Delta\rho)^{1/2}} \quad (1.4); (1.5)$$

1.7 Plug/Churn Transition

A few methods have been developed to describe the plug/churn flow transition. Mishima and Ishii (1984) suggested that the transition between plug and churn flow goes from void fraction limitation. They found the mean void fraction along a gas plug and the mean over the whole plug unit. The transition was described as the condition at which the void fractions were the same. Although their transitions demonstrated good agreement with experiment it is not considered as trustworthy as there was a wrong application of Bernoulli's equation. Taitel et al (1980) thought that churn flow is an initial effect associated with plug regime and have made a model including a length effect. This method suggests that for unlimited long pipes only annular, plug and bubble flows may be and therefore a direct transition process between plug and annular flows is needed. In plug flow, however, the film can travel downwards while in annular flow it goes upward, so an intermediate condition may be predicted between the film downflow and upflow, especially from the data obtained by flooding experiments. Because of that Taitel et al method is not likely to be appropriate. Brauner and Bamea (1986) also applied a limiting void fraction method and suggested that slug flow should change to churn flow if the void fraction in the liquid plugs among the Taylor bubbles become the same with the maximum packing void fraction.

Nicklin and Davidson (1962) suggested that churn flow appeared if the gas flow in the pug is enough to make flooding in the film surrounding it. This method is realistic because it is clear that waves occur on the film towards the end of the gas plug at conditions below the transition. Evidently this is the first sign of the instability which at higher flow rates leads to flooding. Later McQuillan and Whalley (1985) used this theory and obtained a transition criterion. The method was altered by Jayanti and Hewitt (1992) who thought that as there is a considerable effect of film length on the flooding point in counter-current flow, the length of Taylor bubbles should be considered.

1.8 Churn/annular transition

For this kind of transition a few methods also have been reported. Taitel et al (1980). Proposed that the transition may be determined if the gas velocity is just enough to suspend a droplet. They applied the drag equation:

$\frac{1}{2} c_D \pi \frac{d^2}{4} \rho_g u_g^2 = \frac{\pi d^3}{6} g \Delta\rho$ (1.6) The drop size was described the largest the biggest steady droplet which was determined from the formula of Hinze (1995)

$$d = \frac{We_c \sigma}{\rho_g u_g^2} \quad (1.7)$$

Another method links the transition with the flow reversal transition. Different papers have studied the transition in a number of ways. Some of them produced flow reversal experiments, others applied related minimum in pressure drop or visual observations. The results may be described with the help of Wallis parameter:

$$u_g^* = \frac{u_{gs}\sqrt{\rho_g}}{(g D_t \Delta\rho)^{1/2}} = C \quad (1.8)$$

The value for C has been proposed by a number of people. Examples of the pressure drop minimum are illustrated in figure 1.8. It demonstrates that there are some difference in u_g at the minimum for different fluids the value of approximately 1.0, however, is a sensible representation.

Figure 1.8 Minimum in pressure drop. Willetts et al (1987)

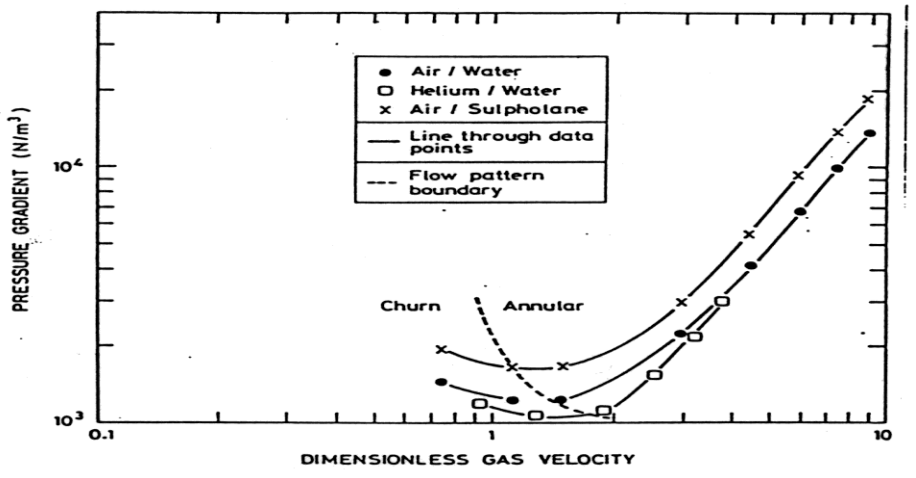

1.9 Horizontal flow

1.9.1 Flow patterns

Here the flow patterns occurring in horizontal pipes are briefly described.

If gravity act perpendicularly to the pipes axis separation of the phases can occur. This increases the number of flow patterns, as shown in figure 1.9

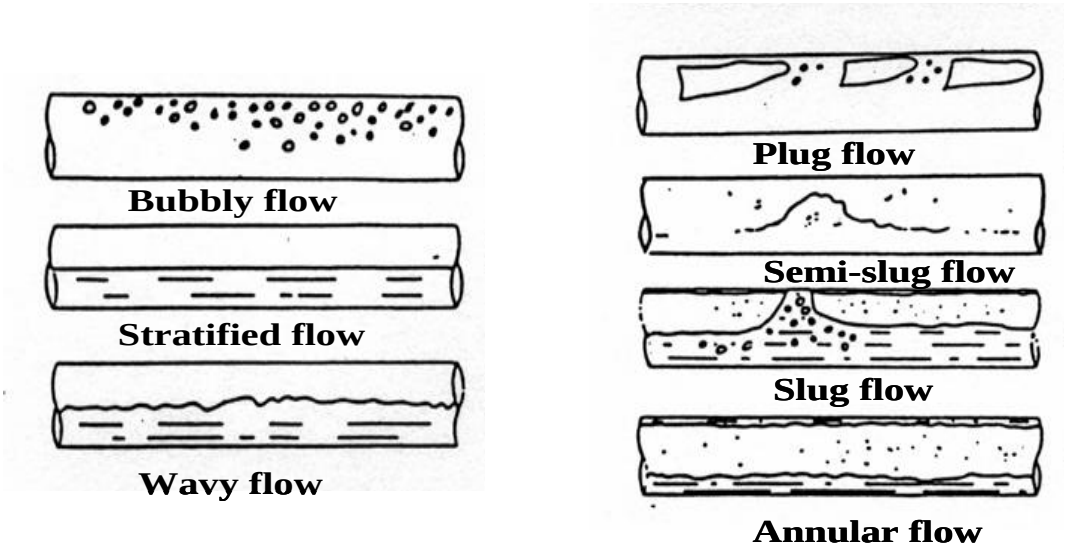

Figure 1.9 Flow patterns in horizontal flow. (Azzopardi 2006)

- Bubbly flow

This flow like it's the equivalent regime in vertical flow presents the gas bubbles dispersed in the bulk of liquid, but except at very high liquid velocities when the turbulence is so high that the bubbles are dispersed in the cross section, the bubbles are collected in the upper part of the pipe due to the gravity.

- Stratified flow

In this case the liquid flows in the lower part of the pipe, gas – above it. The interface between them is smooth.

- Wavy flows

If the gas velocity goes up waves appear on the interface of stratified flow.

- Plug flow

This flow regime can be described as bullet shaped gas bubbles as in vertical flow, but in horizontal flow they travel at the top of the pipe.

- Slug flow

This regime like plug flow is intermittent. The gas bubbles are bigger, while the liquid slugs have a lot of smaller bubbles. When the slugs contain a lot of air, the term frothy surges may be used (Coney, 1974). The term semi-slug is used by some workers to characterize cases where surges do not fill the tube completely (Sakaguchi et al. 1979).

- Annular flow

A continuous gas core with film of liquid on the walls describes this flow regime, liquid can be entrained in the gas core. Gravity makes film be thicker on the lower part of the pipe. However if the velocity goes up the film becomes circumferentially ore uniform.

1.10 Aim

Since the knowledge of multiphase flow in large diameter pipes is limited this study has been carried out. The aim was to investigate effect of physical properties on gas-liquid flow in large pipes over a range of flow conditions. This study will concentrate on the effect of gas density.

1.11 Objectives

Several objectives have been considered to be essential for getting a better understanding of multiphase flow in vertical 127 mm pipe. After obtaining experimental results the following characteristics were investigated:

- Void fraction
- Film thickness
- Frequency

Chapter 2 Literature review on multiphase flow in large diameter pipes

2.1 Introduction

Multiphase flow is very common phenomena in power, nuclear, chemical, hydraulic, metallurgical engineering. For optimization of industrial processes, particularly design and safety issues the physical properties of such flows should be studied and understood. Analysis of recent published papers shows that multiphase flow in larger diameter pipes is of increasing interest. This may be the result of the growth in offshore gas and oil production, as transportation in that case needs relatively long pipe works of big diameter for reducing pressure drop (Omebere-Iyari 2007, 2008). According to Yoneda et al. (2002) the usage of large diameter pipes can significantly improve performance of the equipment in nuclear industry.

It was noticed that although multiphase flow in large diameter pipes is very important and many papers have been recently published on this area, most of the published papers are devoted to smaller diameter pipes (Omebere-Iyari 2008). Thus exploring this area is serious and perspective field of study.

2.2 Multiphase flow in large diameter pipes

Recent papers cover wide range of experiments and investigate different parameters in large diameter pipes. The necessity to investigate certain parameters is motivated by a particular problem or improvement to be made in industry. There have been papers on investigation of bubble characteristics such as size, measurements of void fraction, and observations of flow patterns for the large diameter pipes.

Duan et al (2011) used two types of population balance approach: Inhomogeneous Multi-Size-Group (MUSIG) and Bubble Number Density (ABND) models for estimation of bubbles size, void fraction. Using numerical approach authors evaluated predictions for both models against experimental data from MTLOOP (Lucas et al., 2005) and TOPFLOW (Prasser et al., 2007) in both studies water and air were used to create the flow.

Lucas et al (2005) measured two phase flow using 3.5 m tall pipe with a 51.2 mm diameter. A schematic diagram of the facility is presented in figure 2.1. Liquid was circulated from the bottom to the top of the riser. A constant temperature of 30 ℃ was maintained. Gas was injected through especial device which had 19 holes with inner diameter of 0.8 mm. A wire mesh sensor for measuring the void fraction and bubble size distribution was installed at a certain distance from injection points. The distance could be varied from 30 to 3030 mm (Z/D=0.6–60). A pump and a compressed air source were controlling the flow rates; the maximum superficial velocity for air was 14 m/s, for water 4 m/s.

Prasser et al., (2007) who worked on the TOPFLOW facility was using a vertical pipe 9 meters high and 195.3 mm in diameter, a schematic diagram is shown in figure 2.2. As in MTLOOP experiments water and air were used, the temperature of the water was maintained at 30 ℃. It was circulated from the bottom to the top and the maximum superficial velocities were the same however a different type of air injection was employed. The injection system was variable, constructed by installing air injecting devices at 18 different positions from Z/D=1.1–9.9. Three levels of gas section were installed at every injection point. Two of the sections had 72 round orifices of 1 mm in diameter for tiny bubbles and one section had 32 round orifices of 4 mm diameter for large bubbles. As in MTLOOP study a wire mesh sensor was employed at the top of the riser for collecting the gas volume fraction and the bubble size distribution data.

Using data from these studies Duan et al (2011) produced results via generic computational fluid dynamics code ANSYS-CFX11. It was found that for two gas injection systems bubble coalescence was prevailing in (Lucas et al., 2005) and the breakage of bubbles in (Prasser et al., 2007). Using the experimental data from the two papers Duan et al (2011) assessed performances of two balance approaches – Average Bubble Number Density (ABND) and Inhomogeneous MULTI-Size-Group (MUSIG) models. Each of the models showed good agreement with the measurements.

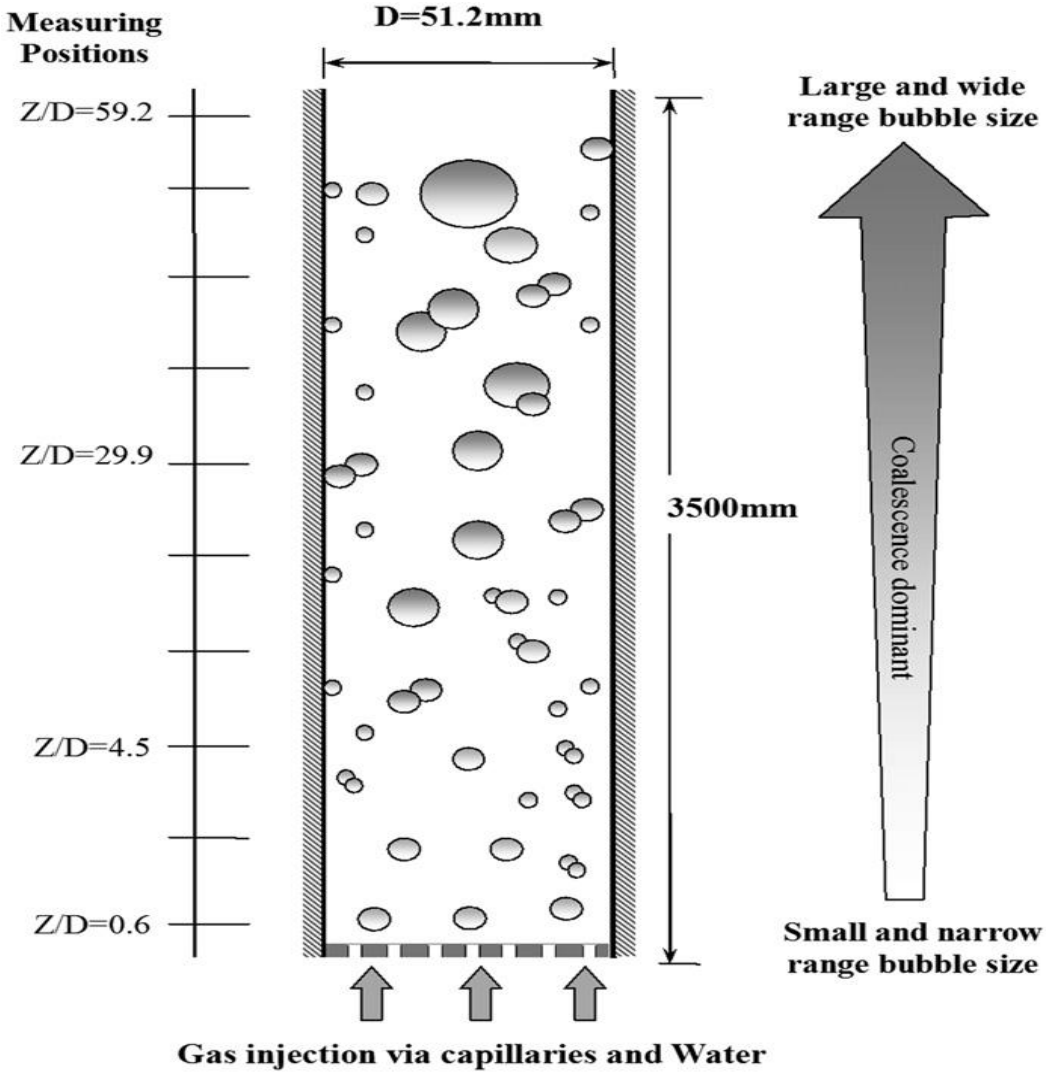

Figure 2.1 Schematic drawing of the test section of MTLOOP experiment, Lucas et al. (2005)

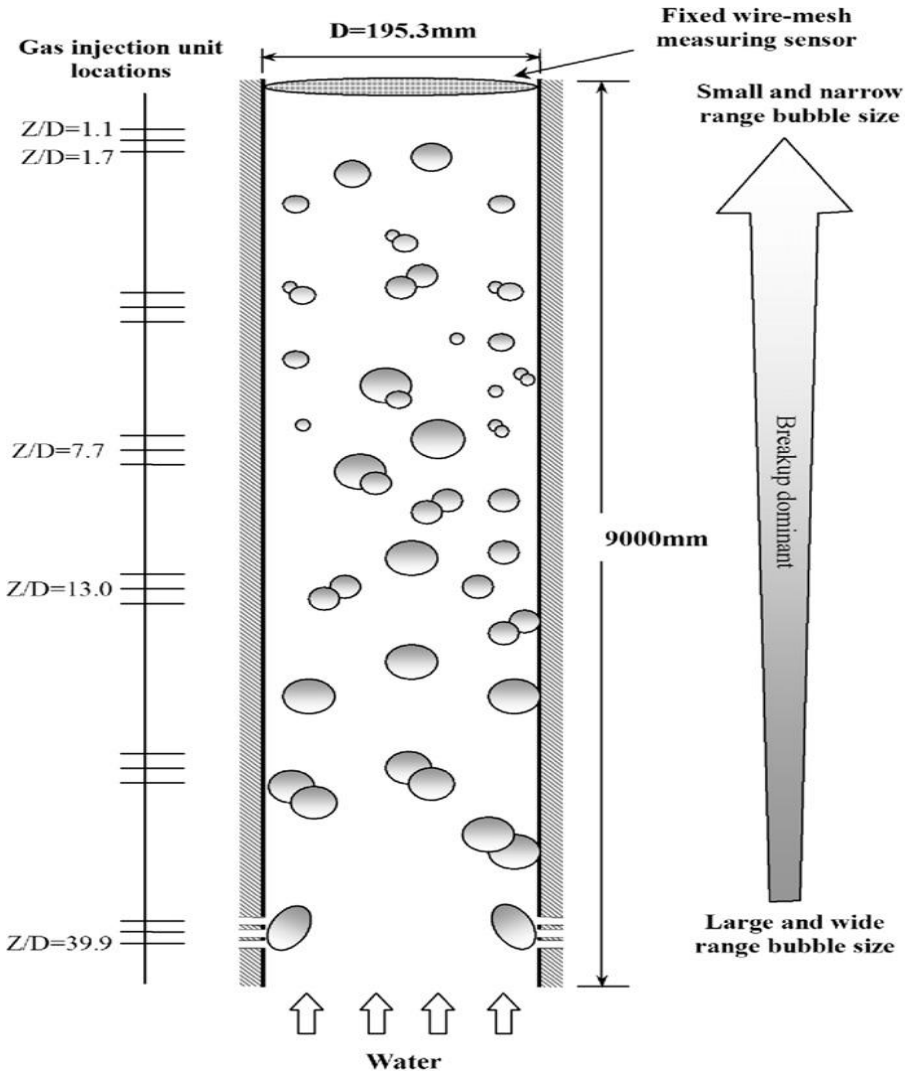

Figure 2.2 Schematic drawing of the test section of TOPFLOW experiment, Prasser et al., (2007)

As in the two experiments different injection methods were employed Duan et al (2011) decided to use a dimensional axial location (Z/D) to present the dimensional physical distance and bubble size development between gas injection and measuring points within the two different experiments. If the Z/D increases different trends of bubble combination and break up appeared in both experiments. In the TOPFLOW experiment with the gas injection holes made on the perimeter of the tube very concentrated bubble were observed within the wall proximity. It was compactly packed swarm of bubbles which then immediately coalesce with other bubbles and became larger bubbles. It can be concluded that this quick formation of bubbles showed a bimodal bubble size distribution with a wide

spectrum of bubble size varying from diameters of 0 to 60 mm. These bimodal distributed bubbles from the injection unit gradually collapsed to the one-peaked distribution at the top of the test area.

Unlike TOPFLOW experiments when bubble breakage is clearly dominant mechanism within the gas-liquid flow, bubble union was observed to be the dominant mechanism in the MTLOOP experiment. With gas bubbles being injected through the 19 identically distributed capillaries these bubbles that were evenly distributed in the tube inlet showed a single-peaked distribution with a quite a narrow number of size between bubble diameters of 2 and 10 mm. While they were traveling upward larger bubbles were further formed through the coalescence which often extended the size of bubbles at the exit of the tube.

The study showed by these observations that in the two experiments, even under the same flow parameters but different gas injection techniques both experiments demonstrated different bubble union and breakage processes, this gave the impulse to properly test the coalescence and breakage centers used in ABND and MUSIG models. The authors found that all in all predictions from both experiments are in good agreement with the measurements

Omebere-Iyari et al (2008) was investigating void fraction and bubble size distribution in large diameter pipes at high pressure – 46.4 bars and 259.3 degrees, using saturated steam and saturated water. These conditions were similar to Omebere-Iyari et al (2007), it was done to be able to compare the data from the two experiments as at the above conditions the gas density and viscosity are equal to the 20 bar experiments of Omebere-Iyari et al (2007), and the liquid density, surface tension, liquid viscosity are 1.2, 1.3, 0.3, physical properties of the fluids are presented in table 2.1. The paper also provides visual images of the gas/liquid flow; they were obtained with the use of a wire mesh sensor. A schematic diagram of the experimental facility is presented in figure 2.3. It should be noticed that the experimental facility is a complicated one with powerful cooler and heater.

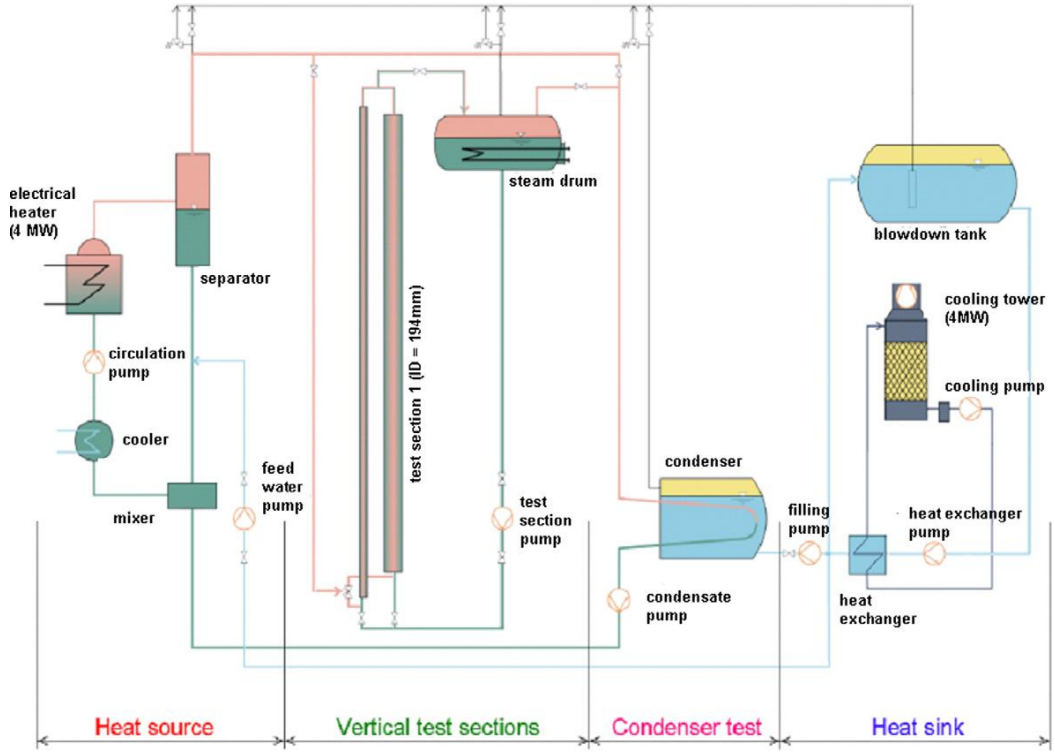

Figure 2.3 Flowsheet of the TOPFLOW facility, Omebere-Iyari et al (2008)

	Units	Omebere-Iyari et al (2008)	Omebere-Iyari et al. (2007)
Fluids		Steam/water	Nitrogen/naphtha
Pipe diameter	mm	194	189
Temperature/pressure	bar/C	46.4/259.3	20/30
Density Gas	kg/m3	23.4	23.4
Liquid	kg/m3	784.9	702.3
Viscosity Gas	Pa s	1.79E-0.5	1.77E-0.5
Liquid	Pa s	1.03E-0.4	3.59E-0.4
Surface tension	N/m	0.0239	0.0185

Table 2.1 Physical properties of the fluids of Omebere-Iyari et al (2008, 2007)

Gamma densitometry technique was employed by Omebere-Iyari et al (2007) to measure phase distribution in the riser. A gamma densitometer possesses a radioactive source, it gives off gamma rays on a side of the tude to be picked up on the other side by ionization type detector. The gamma beams are exhausted differently in liquid and gas, thus the amount of radiation at the detector is affected by phase distribution in the pipe. Authors

used two types of densitometers with broad and single beams. The first instrument was used for cross-sectionally while the second for line averaged void fraction.

Visual images of virtual side projections and side view of the riser showed that conventional slug flow was absent in large diameter pipes, authors noted other studies confirming that - Ohnuki and Akimoto (2000) and Prasser et al. (2005) and studies which are in contrary to this Taitel et al. (1980); Costigan and Whalley (1997), however in the last two studies pipes of smaller diameters were used. The images are presented in figure 2.4. Bubble flow is small bubbles in the liquid flow while churn-turbulent flow is characterized by big bubbles the length of which is much larger than diameter of the pipe.

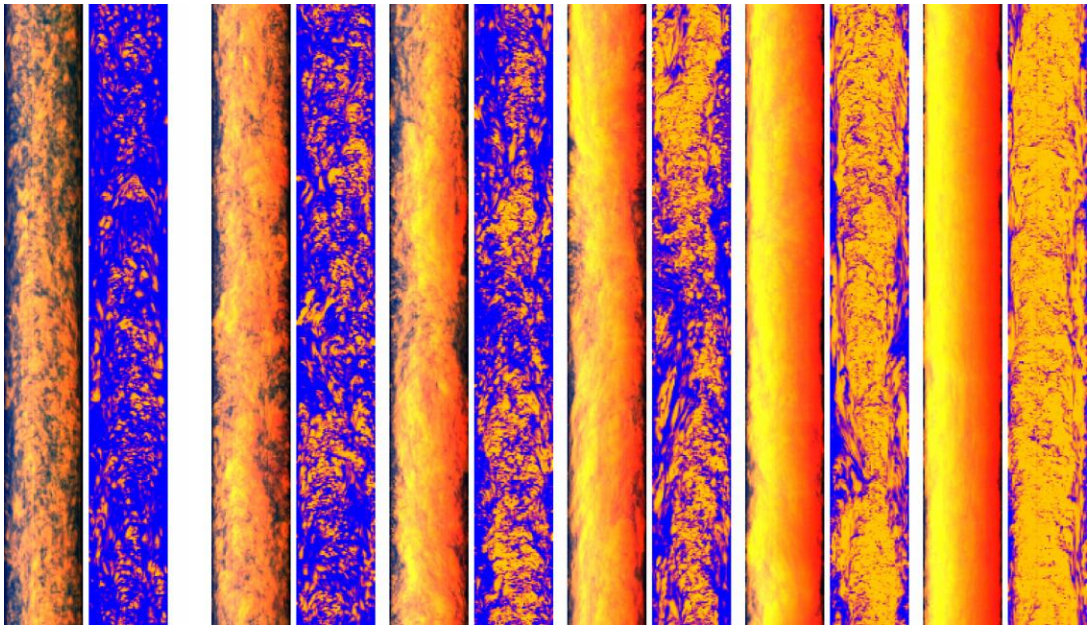

A) B)

Figure 2.4 Side projections (a) and sectional side views (b) for liquid superficial velocity 0.01 m/s, Omebere-Iyari et al (2008)

Figure 2.5a presents small bubbles distributed in the liquid at the smallest flow rate, when the bubbles become more irregular and bigger the flow pattern changes to churn-turbulent, figure 2.5b

As in case of Prasser et al., (2007) the experiments were done in TOPFLOW (transient two phase flow) rig. Water flows from the steam drum to the riser moved by the pump. The steam is generated in the heating equipment: electro heater, pump, cyclone separator. Multi-strand nozzle meter with the maximum error of 1 % was employed for flow

measurements. Steam was put into the test section through a special mixing section and holes at the bottom of the riser, after the mixture flows up, and the gas separated from the water in the steam drum. The rig possesses wide range of injection methods for investigating the flow, schematic diagram is presented in figure 2.6.

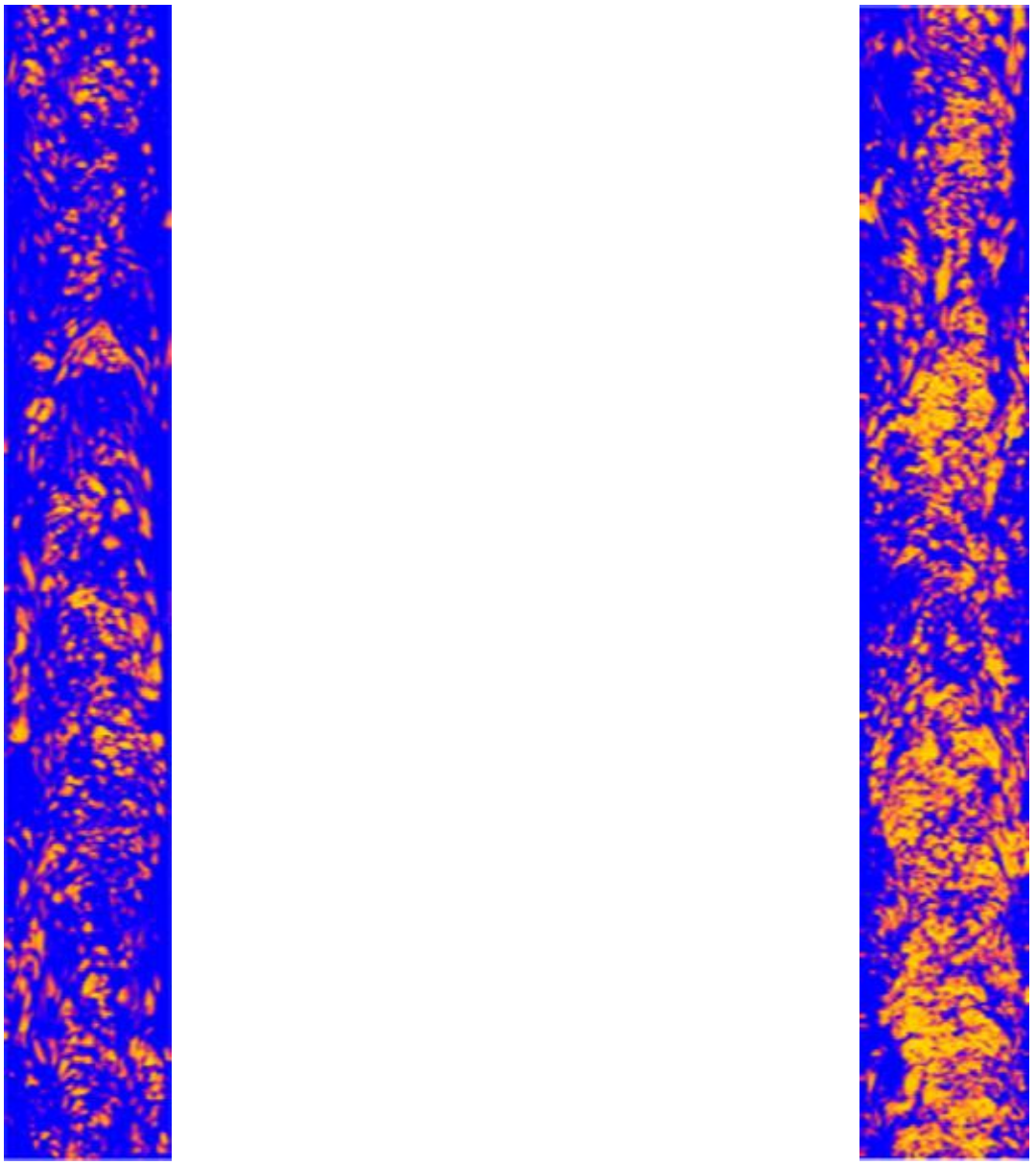

A) Bubbly flow U_{gs}=0.09 m/s B) Churn-turbulent flow U_{gs}=0.20 m/s

Figure 2.5 Flow patterns images obtained with the use of wire mesh sensor, at the liquid superficial velocity of 0.01 m/s, Omebere-Iyari et al (2008)

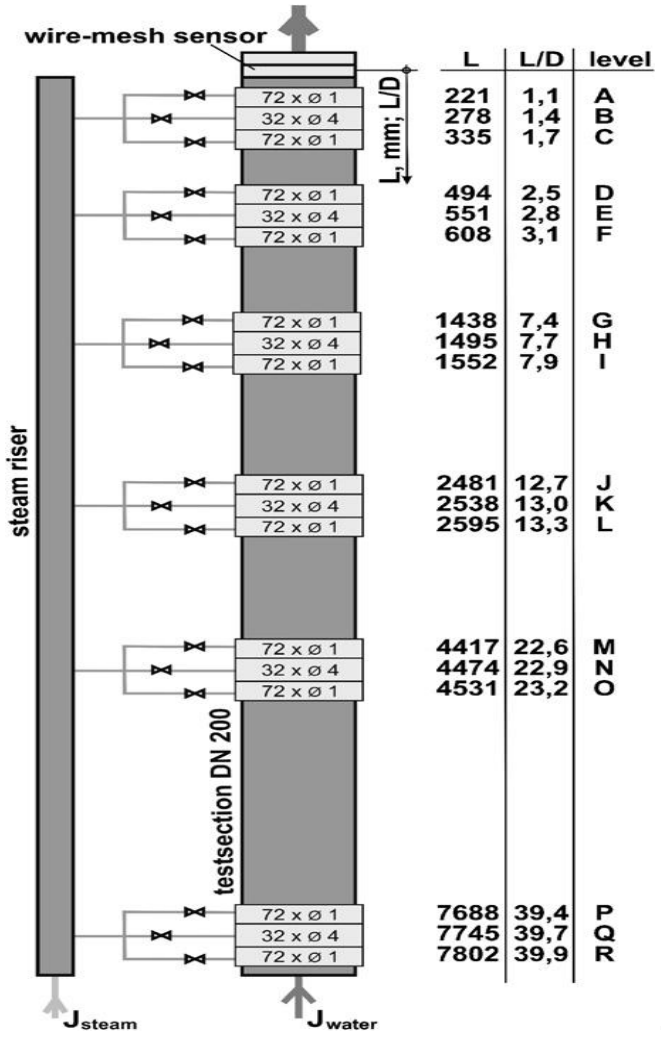

Figure 2.6 Schematic injection diagram of the TOPFLOW, Omebere-Iyari et al (2008)

In Omebere-Iyari et al. (2008) measurements were produced at exactly the same inlet phase velocities as some of the experiments from Omebere-Iyari et al. (2007). The maximum gas superficial velocity in the later work was 1.5 m/s because of some restrictions in power supply due to the steam generation. A heat balance of the flow streams has been required to find out the real flow rates of the gas and liquid phases at the wire mesh sensor. This was to take into consideration the condensation which occurred while the mixture was traveling in the pipe. The calculation was carried out by using the inlet temperatures, flow rates, pressures and the temperature and pressure at the wire mesh sensor. The heat loss

has been taken as 4 kW; this is a very small value in comparison with to the enthalpies involved and the authors found that the effect of it could be neglected. The following results of the flow development were observed: at L/D ratio of about 40 the experiments were fully developed, this is in agreement with Prasser et al (2005) who found that two phase flow of water and steam at 65 bar pressure converges much faster than air/water mixture under atmospheric pressure. This, however different from Omebere-Iyari et al (2007) who observed that an L/D of 157 is needed for fully developed flow of a mixture of nitrogen/naphtha in tubes of similar size.

Cross-sectionally averaged void fraction. The time varying void fraction and PDF plots for steam and water have been compared with nitrogen/naphtha data at similar phase velocities. Reasonable agreement was observed between void fraction values at the liquid superficial velocity of 0.65 m/s for both sets of experiments, but considerable and methodical difference at the lower liquid superficial velocity of 0.1 m/s was found.

Line averaged void fraction. The two papers obtained similar data on line averaged void fraction Omebere-Iyari et al (2007) with single beam gamma densitometers and Omebere-Iyari et al (2008) with wire mesh sensor. It was found that the mean void fraction for both axes is equivalent for both measurement instruments.

Authors investigated void fraction, distribution of bubble size, flow development and patterns. A number of conclusions were drown out of the experiments, the most important of them are: there is no slug flow in a large diameter pipe for steam/water flows at high pressures; converging of steam/water at high pressure happens much faster than in case of air/water at the atmospheric pressure; void fraction of air/water is different from nitrogen/naphtha for the same vertical pipe, influences the coalescence of bubbles.

The same Transient Two-Phase-FLOW test technique (TOPFLOW), was used by D. Lucas et al (2010), the authors obtained data base of air/water flows. Again variable gas injection test section was employed it was a vertical steel tube with the diameter 195.3 mm and length 8m. Six gas injection devices provided the possibility of to inject gas through holes in the tube wall.

The measurement instruments were also a wire mesh sensor and a high speed camera for evaluation of the error of measurements for the volume equivalent diameter of bubbles. The experiments were done at the constant pressure – 0.25 Mpa and temperature 30 degrees. The measurements were produced at 48 different combinations of water and air superficial velocities, changing from 0.04 m/s to 16 m/s for water and 0.0025 m/s to 3.2 m/s for gas. The data obtained was used to calculate the distribution of bubble size and

other time-averaged parameters. The authors observed that bubble size distribution goes down with the increase of diameter, did observations of void fraction, identification of single bubbles. Attention was also paid for estimating the plausibility of experimental results, the data obtained from wire mesh sensor was checked with the use of gamma measurements and X-ray tomography.

According to Oddie et al (2003) very few papers are available on three phase flow in large diameter inclined pipes, the authors tried close the gap in this area doing experiments with the following materials: tap water, nitrogen and kerosene creating two and three phase flow. Authors highlight the importance of understanding of the interactions happening in the petroleum reservoirs, interactions between reservoir and wellbore, the goal of the paper is to validate and improve wellbore flow models. The experimental facility is designed with the purpose to be able to investigate the whole range of upward flows from 0 to 90 degrees.

Apart from usual measurement instruments as flowmeters and thermometers, more specific instrumentation was employed: video cameras, gamma densitometer, hydrophone, electrical probes. Varying different parameters as flow rates, angle of inclination of the pipe, many flow patterns were observed: churn, slug, stratified wavy, stratified, bubble, elongated-bubble. Figure 2.7 shows the flow patterns at different angles.

Hold up was measured using three techniques: shut-in – the classic method and is thought to be one of the most reliable methods. The whole test section was used as the shut-in zone, such shut-in method is good for transient flow, however entrance and outlet affection to the holdup measurements. Probe identify momentary fraction of liquid in the pipe, and thus may be used to find holdup. Nuclear holdup: the densitometer is installed in a place where the flow is not affected by the entrance or outlet effect. The results from each method were compared for more accuracy. Despite the fact that the methods have some inaccuracy, especially nuclear and probe techniques, the three methods showed reasonable agreement with each other.

The flow patterns observed were compared against predictions of mechanistic model of Petalas and Aziz (2000). It was found that the mechanistic model in good agreement with observed flows. However authors call this agreement is ”somewhat surprising” as mechanistic model was developed using data obtained in pipes with diameter <5 cm. A thorough literature review is also an advantage of this study.

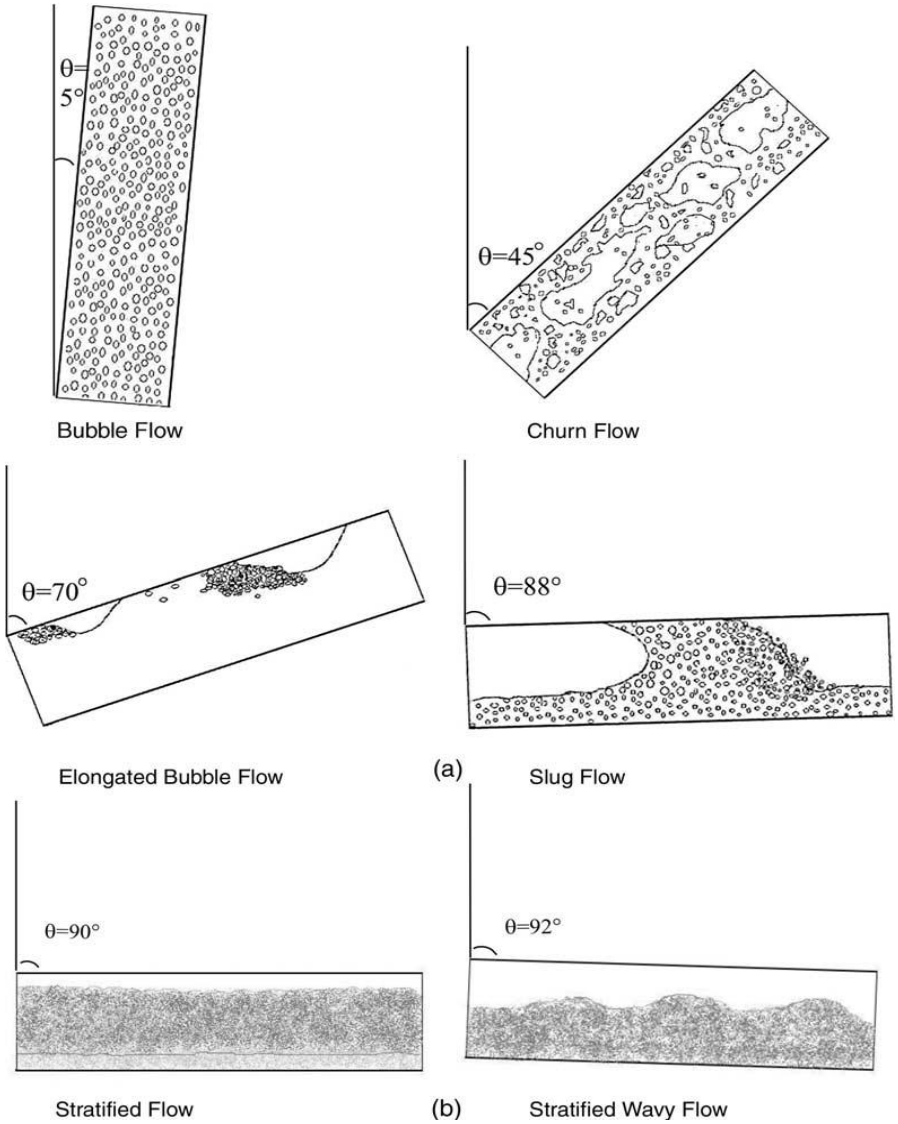

Figure 2.7 (a) Some of observed water-gas flow patterns with typical inclinations, (b) some of oil-water-gas flow patterns obtained with typical inclinations, Oddie et al (2003)

Yan-Bo Zong et al (2010) did another study of multiphase flow in inclined pipes of large diameter using tap water and No 15 industry oil, the oil density was 856 kg/m^3, viscosity was 11.984 MPa s (40C) and surface tension was 0.035 N/m, the water was colored red for the convenience of visual observation.

Characteristics were investigated with the help of the vertical multi-electrode array (VMEA) conductance probe and mini-conductance probes. The experimental facility of 6 meters high and with diameter 125 mm has the possibility to be inclined from 0 to 90 degrees, electromagnetic flow meter and calibrated turbine were used to measure flow rates

of oil and water. VMEA and mini conductance probes were connected to the test section at 3 m from the inlet. Figure 2.8 represents experimental facility of inclined oil-water flow.

Figure 2.8 Schematics of inclined oil–water two phase flow experiment, Yan-Bo Zong et al (2010)

The disription of VMEA sensor and mini condactance probe array is taken from Wang 2010. VMEA sensor is constructed by the electrical impedance tehniques for flow measurements. The instrument is made of eight stainless steel ring electodes of the material $Cr_1Ni_{18}Ti_9$, that is installed inside of the acrylic pipe with 125 mm ID and separated into 4 pairs. E1 and E2 are excitation electrodes and connected with a 20 kHz sinusoidal signal. Sensor A and B are the upstream and downstream sensors and used to measure the axial speed. For the phase volume fraction sensor C is employed. The remaining three pairs are to be demodulated with the help model composed of differential amplifier, phase – sensitive demodulator and low pass filter. Figure 2.9 shows the structure of VMEA sensor.

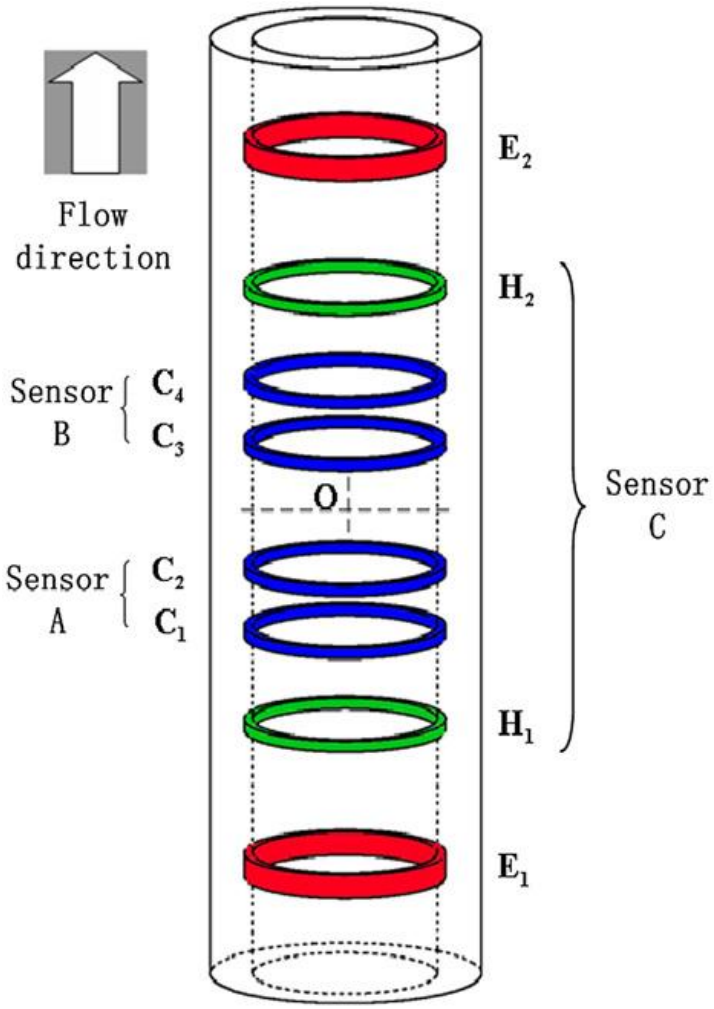

Figure 2.9 The structure of VMEA sensor. Wang 2010, Yan-Bo Zong et al (2010)

The evaluation of local oil-water two phase flow patterns, mini-condactance probe array was used to identify the continious liquid. The probe is made basicaly by the bare needle electrode and conductive casing is activated by +5 V voltage and the needle electrode works as measurement port. If the needle electrode is covered by conductive media – water, the circuit is formed amid needle electrode and casing, and output signals are at small voltage; if the needle electrode is covered by the non-conductive liquid, the circuit is disconnected and the output signals are at high voltage. The authors refered Jin et al., (2008); Zheng et al., (2008) as the source for more details of data acquisition systems.

For the water and oil superficial velocities from 0.0052-0.3306 m/s with angles of inclination of 15 and 45 degrees authors studied usual for oil and water flow patterns:

dispersion of oil-in-water pseudoslugs, dispersion oil-in-water countercurrent, transitional flow and dispersion of water–in-oil flow. High speed camera helped to precisely identify different flow patterns at variety of conditions.

Analyzing the data collected authors provide flow patterns maps, employing quantification analysis and attractor geometry morphological description method, signal time series measured from VEMA sensor were analyzed and good flow pattern classification was achieved.

Using the same experimental facility, the same measurement instruments VMEA and mini-conductance probe array, oil with the same characteristics and same water with Yan-Bo Zong et al (2010) a study of three phase flow was done by Wang et al (2010). The authors investigated dynamical characteristics of oil-gas-water three phase flow, using nonlinear time series analysis. The experiments were done in 125 mm pipe. The total flowrate was smaller than 300 m^3/day the, the oil to total liquid flowrate coefficient (f_o) was varied from 0.1 to 0.95. At the beginning liquid flowrate (Q_w) and oil flowrate (Q_o) were constant, f_o at the minimum, then gas flowrate (Q_g) was gradually grown, when one f_o was investigated another f_o was increased, thus the three phase flow data for a number of f_o was collected. This experimental method was convenient to observe gas-liquid flow pattern transition trend influenced by the oil for f_o and the effect of gas on oil-water flow patterns and the phase changing of liquids for high f_o in the same total liquid flow rate. The following total liquid flowrates were studied 20, 40, 60, 80 m^3/day, f_o were 0.1, 0.2, 0.3, 0.4, 0.5, 0.7, 0.9, and gas flowrates ranged from 8 to 180 m^3/day. 235 flow conditions were observed.

The data obtained was used for making flow pattern maps. The analysis of flow pattern maps showed that: the growth of the ratio of oil flowrate to the total liquid flowrate (f_o) creates oil in water type slugs at low gas superficial velocity; for big diameter pipe and low flow velocity, the phase inversion of liquids happens at around f_o and the disturbance of gas makes the inversion point move to low f_o. Authors used attractor shape of the signals received from VMEA sensor for identifying the four observed flow patterns by utilization two attractor morphological characteristic. Using the signals obtained with VMEA sensor two complexity measures were developed Lempel–Ziv complexity (Lempel, Ziv, 1976) and Approximate entropy for studying the dynamical parameters of different flow patterns.

Xiuzhong Shen et al (2010) studied the distribution parameter and the drift velocity for two phase flow in a vertical large diameter riser. Figure 2.10 shows the schematic

experimental loop, purified water and air were used to create two phase flow, water was substituted every day while the experiments were in progress to keep the liquid phase quality. Water was in the lower tank and was moved by a pump. For adiabatic air-water experiments porous sinter pipes with diameter 40 micro m were employed as the gas injections. The water was lead through Venturi flow meter, was separated into four flows, then mixed with air in the mixer. The water that was pumped through another Venturi flow meter was separated into two streams and then mixed with the former air-water stream before the mixture was injected into the riser. After going through the test section the phases were separated from each other in the separator. The temperature of the water was maintained constant with deviation of 1 degree for every experiment. The test section was made of stainless steel, because of high pressure. Pipes used in the experiment were 200 mm in diameter, the height of the riser was around 25 m.

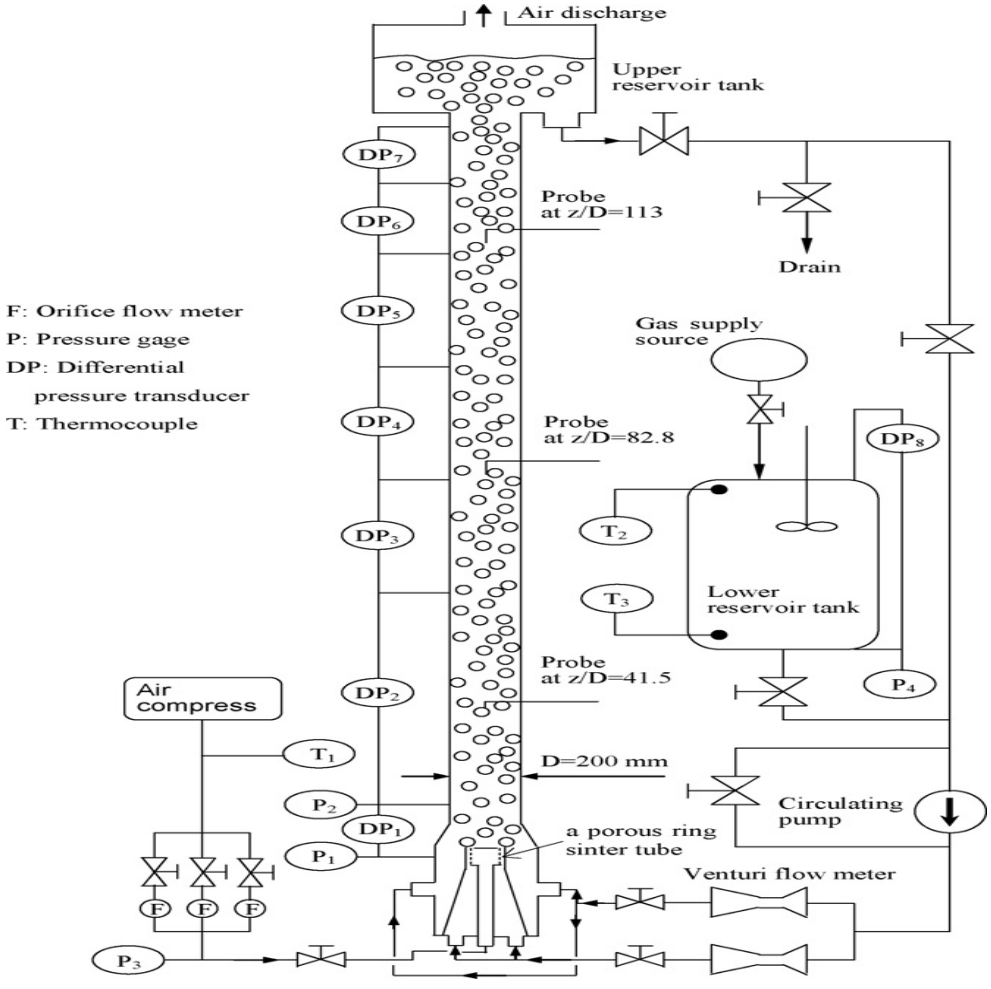

Figure 2.10 The sheam of the experimental loop, Xiuzhong Shen et al (2010)

Optical multi sensor probes , i.e. flat-tip optical four sensor probes were connected at 3 axial locations of Z/D=41.5, Z/D=82.8, Z/D=113 to acquire the void fraction and gas velosity data. Experiments were produsedat 11 radial positions to receive local characteristics of adiabatic air–water two phase flow. The We7000 control data acquisition system together with optical probes was employed for collecting the data. Dantec 55R61 X-hot film probe measured the upward and circumferential turbulent velocities in the flow. The hot-film probes were traversed in the radial direction in the same manner as optical probes. Measured data was collected using NI PCI /AT-MIO-16E-1A/D board.

The work of optical probes is based on the refraction and reflection laws. Multiphase flow passing the probe makes the laser light to change from one reflection form to another, in this way the presence of liquid or gas near the tip can be identified in the flow. The time averaged local void fraction is measured using the ratio of the accumulated time when the tip is in gas phase to the whole sumpling time. A four-sensor probe is made of one sensor at the front and three sensors at the rear. The void fraction at the front sensor is normally employed as the representative paramenter of the four probe sensor. With the assumption that the gas superficial velocity is the same with the interfacial velocity and the bubbles flow parallel to the sensor probe direction it is possible to approximate the interfacial velocity by the use of the ratio of two sensor tip separation to the time difference when the interface passes two sensor tip in each double sensor probe. Ultimately the average value of the interfacial velocities from the three couples of accesible pairs (if the bubble fails to meet one or two of rear sensors) is considered as the measured gas velocity of the-four sensor probe. The result of that is knowledge that the measured gas velocity is not trustable, if the lateral bubbly flow dominates in the two-phase flow.

The hot-film anemometer – CTA (constant temperature anemometer) measueres phase velocity by identifying the change in heat transfer from little, electrically heated element – sensor emerged in the fluid. In the CTA the coolng effect is caused by the flow touching the element. The cooling effect is balanced by the electricity goimg to the element in order to keep constant temperature at the instrument.

The experiments were done under the following conditions: the superficial gas velocity varied from 0.0016 to 0.093 m/s and the superficial liquid velocity from 0.051 to 0.311 m/s. Three flow regimes were observed: bubbly, churn and slug. The bubbly flow was obtained at

low superficial gas velocities or at high liquid superficial velocities, it was always evolving in the main flow direction. The bubbly flow is described as small distributed bubbles going up with or without local irregular bubbly motions. The churn flow appeared at low superficial liquid and high gas superficial velocities. The flow was forming at the beginning of the test section at relativetly low superficial velocities. The churn flowis described by the presence big deformed bubbles disturbing the flow and producing strong local turbulence. The slug flow regime was formed at high superficial gas velocity and developed from the bubbly and the churn in the upstream flow section. The slug flow is characterized by the presence of large coalescent cap bubbles. Figure 2.11 shows the flow patterns observed.

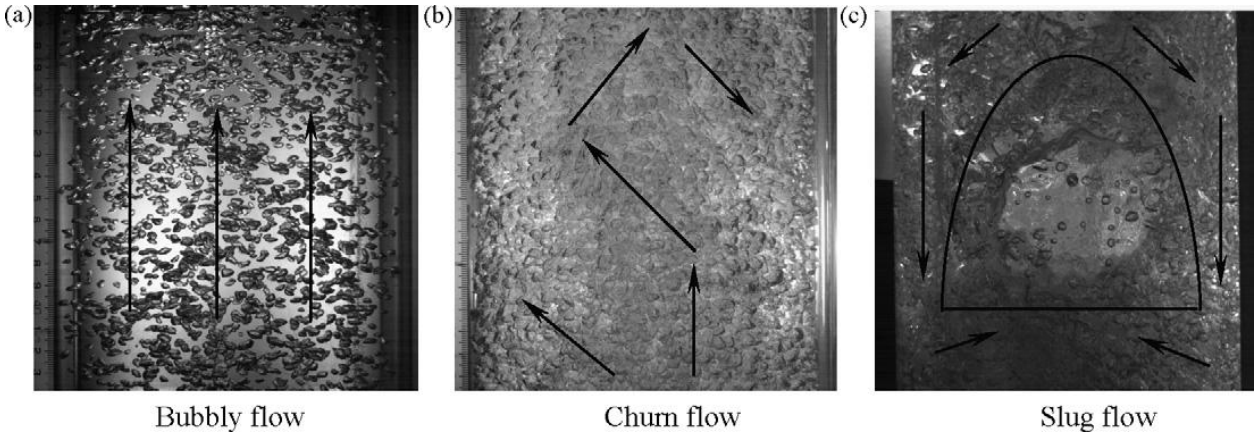

Figure 2.11 Images of the observed flow patterns, Xiuzhong Shen et al (2010)

The data obtained was used to acquire the distribution parameter and the mean drift velocity straight from their definition. The experimental results were compared against predictions of different drift flux correlations.

Schlegel et al (2009) studied void fraction characteristics in two phase flow in large diameter pipes. The authors saw importance of studying the characteristics of two phase flow in large diameter pipes because slug flow does not occur in them, this may be used for designing new nuclear reactors as these designs have a large diameter chimney to enhance natural circulation. Natural circulation is based on difference in density between the hot and or two phase mixture in the chimney and cold water in the downcomer, chimney sustains the gravity head essential to provide natural circulation through the reactor centre. Thus it is

important to have reliable models for the prediction of two phase flow in such systems. The prediction of void fraction in large diameter pipes is essential for the analysis of possible accidence, as void fraction is an important part in the determination of the liquid inventory in the reactor pressure tank.

The experimental facility is presented in figure 2.12. Authors used water and air to create the two phase flow. Water was kept in two separator vessels with total volume of 5680 L. The water was de-ionized water with the addition of morpholine and ammonium hydroxide to adjust conductivity and PH. The pump circulated the water with the maximum liquid flow rate of 0.177 m^3/s. A globe valve after the pump discharge was employed to control the liquid flow rate, which varied from 0.05 to 1 m/s in this study. After, the liquid was lead into a distribution manifold where the temperature was registered and the flow was separated into the main and the secondary liquid flow, each of them then flowed into the injector unit. The unit is shown in figure 2.13.

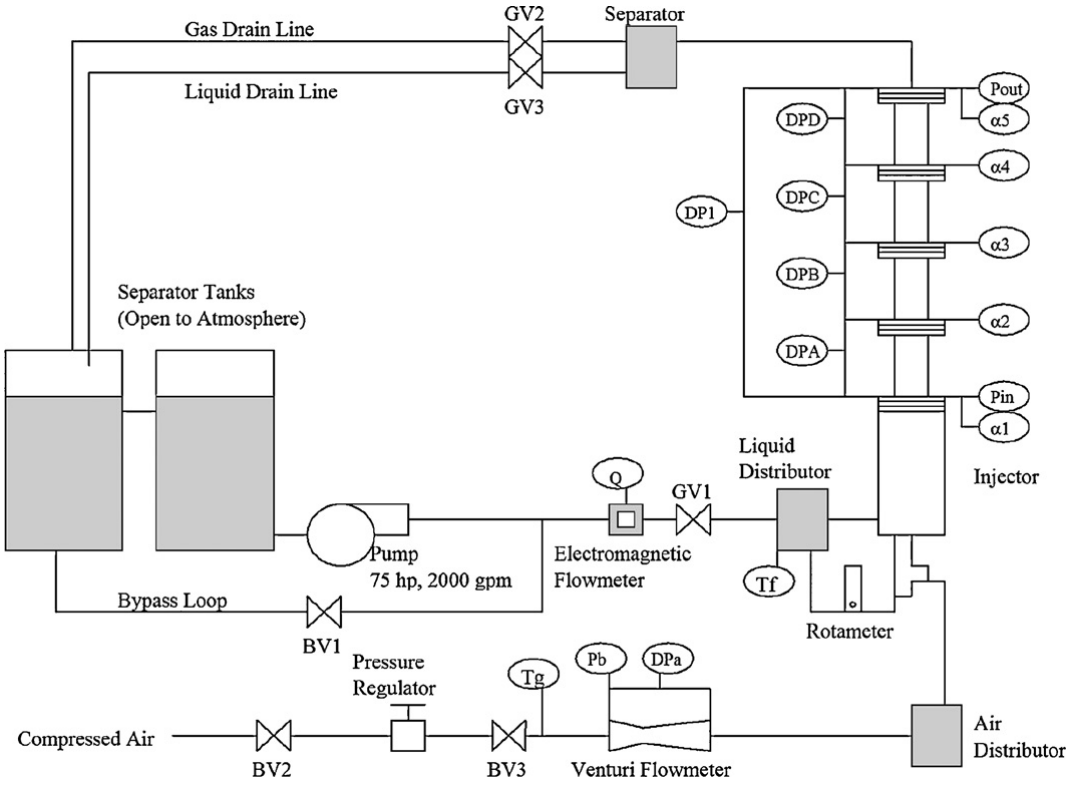

Figure 2.12 The schematic diagram of the experimental loop, Schlegel et al (2009)

The main stream flowed into the injector unit and up into the test section, while the secondary stream flowed into the annuli round air injectors. Those air injectors have a porous metal sparger. By controlling the liquid flow rate through the annuli the initial bubble size may be controlled. Compressed air was provided at 80 psi from an air compressor, the flow rate was controlled with the use of series of ball valves and Venturi flow meters. The gas superficial velocity was varied from 0.1 to 5.1 m/s.

The test section is made of clear acrylic with inner diameter 0.15 m and 4.4 m in length. Measurement points consisted of an impedance meter and pressure tap were installed at Z/d of 0, 7.0, 16.0, 23.0, 29.0. It was revealed that the stainless steel injector intercrossed with the measurements of the impedance probes at D/Z of zero, thus the data from that point was not considered. The void fraction measured was from 0.02 to 0.83. The pressure was monitored using 3051S pressure transducers with accuracy of 0.025 presents of the span.

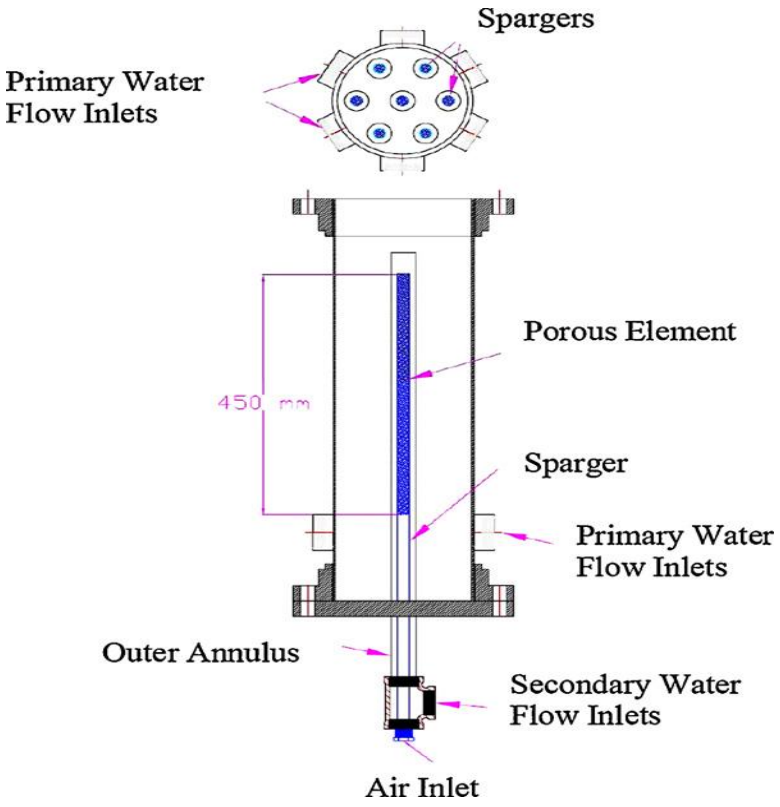

Figure 2.13 The scheme of the injection unit, Schlegel et al (2009)

The volumetric flow rate was measured with the help of an electromagnetic flow meter. This kind of flow meters uses the polarity of water molecules by measuring the distortion in the electric field produced as the water molecules move through it.

The main instrument in the study was electrical impedance void meter. The impedance void meter measures admittance of the two-phase mixture in the measurement area which is recorded as voltage output from the impedance meter circuit. The voltage is then normalized, with 0 meaning that only air is in the test section and meaning that only water fills the test section. Data is collected with a sample rate of 1 kHz for 30 s. This gives very precise measurement of the void fraction without the use of intrusive instruments. Hence the relationship between void fraction and voltage is quite complicated and depends on the flow pattern each void meter is cross calibrated against the void fraction measured by differential pressure. The calibration is carried out at very small liquid velocity, where the frictional pressure drop is less than 2 % of the total pressure drop. Because of that, the accuracy of the impedance probe calibration was depended on the accuracy of the pressure transducers employed in the calibration and the electrical properties of the circuit. All in all the relative error in the void fraction did not exceed 10% of the measured value for the void fractions between 0.2 and 0.4 and not much than 5% for void fraction above 0.4

The authors used the electrical impedance void meter as it does not change the flow development whilst intrusive instruments (wire mesh sensor, local probes) can do it. However the authors noted that intrusive instruments provide more accurate and deeper insight into the mechanics of the flow. The measurements were done at several points simultaneously, it was highly desired that to employ a non-intrusive method. As the intrusive instruments affect the flow it was desirable to avoid the use of them in these conditions. Furthermore, the wire mesh sensors require considerably more data collection capacity and more complicated software than impedance meters. This means that more impedance meters can be employed at the same time in the experiments with the same number of data collection equipment. The authors argued that the accuracy of impedance probe technique (5%) is not much different from wire mesh sensor which is between 1% and 4% according to Prasser 2005(a). The wire mesh sensors need a relatively long time to collect the data, while the impedance probe is able to collect accurate data with time scales of about 0.1 s and flow regime parameters data with the time scale of about 1 s. Because of that if coupled with a properly trained Self Organized Map or neural network, impedance

probes can obtain almost instantaneous data using a very small amount of computing power.

The determination of flow pattern was done by an artificial neural network. Kohonen Self Organized Map (SOM) created by Mi et al (2001) was the base of the neural network used. The authors did some improvements. The Cumulative Probability Density Function (CPDF) of the area averaged void fraction signal was used instead of the Probability Density Function (PDF). The CPDF is an integral value and thus is much steadier than PDF. The CPDF is constantly going up and has a lower input data need. It is also much quicker and easier to extract the CPDF from the raw data rather than PDF. These features make the task easier and increase the ability of the SOM to differentiate the flow patterns. In the experiment 100 points were needed as in CPDF patterns in large diameter pipes the differences in the CPDF between flow regimes are quite delicate.

Authors observed bubbly, cap-bubbly, churn flows and performed comparison of obtained data with experiments of Baily et al. (1956) and Hills (1976). It was found that for void fraction greater than 0.3 the data was in an agreement with their data. The lower void fraction tends to follow the prediction of Hibiki and Ishii (2003)

Another interesting work was done by Zangana et al (2010). The authors studied the effect of gas and liquid velocities on frictional pressure drop in large diameter vertical pipes. Zaganda's et al paper is especially important for this thesis because the same rig was used in both works. A schematic of the experimental facility and description of it work are presented in the next chapter.

Pressure drop measurements were done with the help of an electronic differential pressure detector transmitter, with the range of 0 – 37.4 kPa, and output voltage from 1 to 5 V, a resolution of 9.5 kPa pre volt. Two pressure tappings between which was an axil distance of 12.9 pipe diameters across the transparent section were connected to the differential pressure device via stainless steel pipes. The pipes were filled with water to make the density constant. This was ensured by an efficient purging procedure which excluded the risk of gas fractions in the pressure lines, this was reiterated before starting each set of experiments.

Wall shear stress was measured by hot film probe. It was calibrated by measuring the frictional pressure drop in a single phase flow using an electronic differential pressure

transmitter with a range of 0 – 6.23 kPa and an output voltage from 1 to 5 V. As the wall shear stress is comparatively higher than that in a single phase flow the calibration was done in a high liquid flow rate with positioning the probe in the same location as it was during the experiments owe to sensitivity its sensitivity to its location. The hot film probe is based on heat transfer, therefore the changes in temperature of the system can considerably alter the results.

Liquid holdup. The conductance probe rings were employed for phase distribution measurements were positioned at 62.7, 63.5, 65.5 pipe diameters from the base of the riser. The acquisition of the data was done with the help of a computer equipped with Labview software.

600 of experimental runs were done obtaining pressure drop and liquid holdup for a range of liquid (from 0.01 m/s to 0.7 m/s) and gas (from 3 m/s to 16.25 m/s) superficial velocities. The pressure of 2 bar was set. The frictional pressure drop was acquired from the total pressure drop and the liquid hold up using the steady momentum equation for vertical upward annular flow:

$-\frac{dp}{dx}=F_{wL}+((1-\beta)\rho_G+\beta\rho_l)g$ (1) (2.1) (Sawai et al 2004), here β is the liquid hold up, g is gravitational acceleration, ρ_G and ρ_L are densities of gas and liquid respectively, F_{wL} is the frictional pressure drop and is described by:

$F_{wL}=\frac{4}{d}\tau_w$ (2.2) d is the inner diameter of the pipe τ_w is the wall shear stress.

The time averaged total pressure drop and frictional pressure drop are presented in figures 2.14 and 2.15.

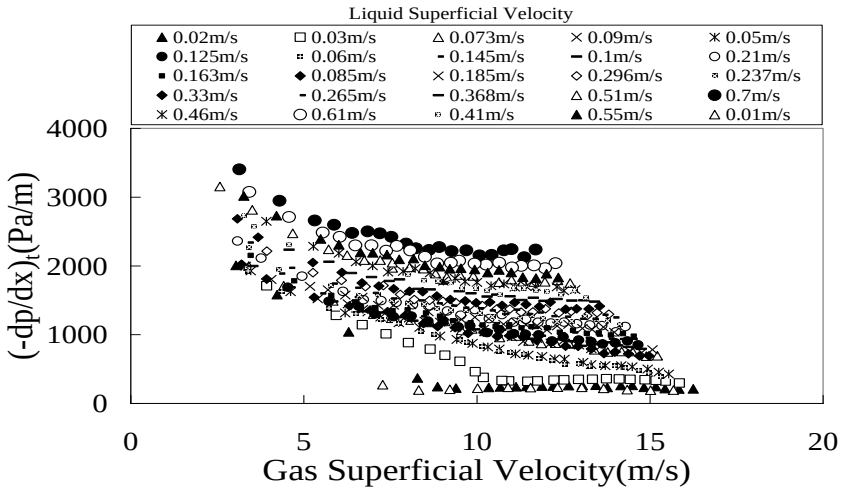

Figure 2.14 Time-averaged pressure drop as function of superficial gas velocity, Zangana et al (2010)

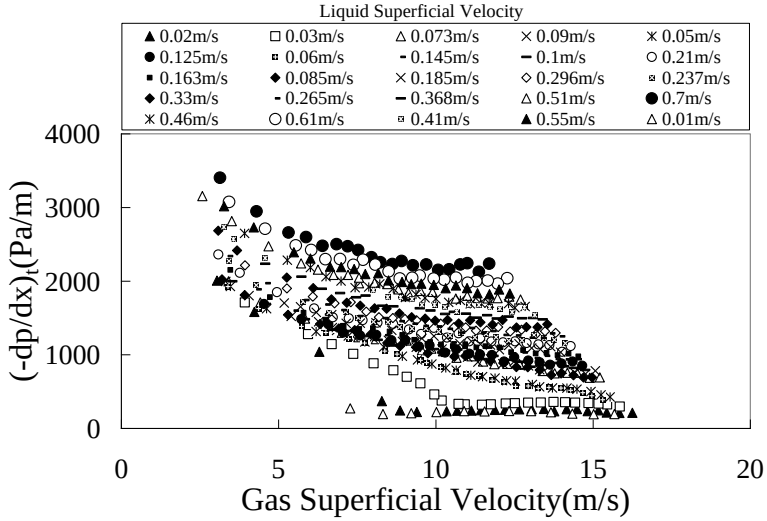

Figure 2.15 Frictional pressure drop as function of superficial gas velocity, Zangana et al (2010)

The authors found three major areas from the figures which were the result of gas and liquid superficial velocity changes. The first area was at low liquid velocities (0.014, 0.02, 0.0 m/s). Here the total pressure decreases dramatically with the increase of gas superficial velocity, then there a gradual decline in pressure drop appears as the gas superficial velocity

increases after going through a possible churn-annular transition region without clear minimum pressure drop. The frictional pressure drop behaves in a similar way over the described range of liquid superficial velocities.

Next region can be described by two particular conditions – o.o5 and 0.06 m/s for the liquid superficial velocity. In this region the trend of frictional and total pressure drop have a smooth appearance.

In the third region the trend was more complex with increasing liquid superficial velocity (from 0.07 to 0.7 m/s). Both total and frictional pressure drop become higher as the liquid superficial velocity goes up.

The authors pointed out the remarkable fact that the liquid superficial velocity significantly affects the frictional pressure drop. It was shown that frictional pressure drop is much lower for smaller liquid superficial velocities. Negative and positive values in the fluctuating frictional pressure drop were obtained at high gas superficial velocity, the authors described this as an "unexpected".

2.3 Conclusion

This review has considered multiphase flow in large diameter pipes. Experimental facilities, measurement techniques, instruments, their working principles, methods of data acquisition and analyzing, conditions of experiments, areas where authors did not agree were shown, compared and contrasted.

Authors of the papers observed that despite the fact that many papers have been devoted to the multiphase flow in large diameter pipes there is still lack of available literature on this area. In order to obtain more knowledge of multiphase flow in large diameter pipes authors employed different techniques varying working materials, measurement instruments, however, most of them have not tried to do the experiments at different pressure and therefore at different density. Thus this work attempts to fill the gap in this area.

Chapter 3 Experimental facility

In this chapter the experimental facility employed is described. The rig was built in the School of Chemical and Environmental Engineering of the University of Nottingham. After the description of the facility the measurement instruments and the experimental conditions used are considered.

3.1 Flow loop with 127 mm diameter riser

A schematic diagram of the facility is presented in Figure 3.1. This rig is of a "Double Closed Loop" configuration, where both of the fluids (air and water) are isolated from the atmosphere: so the rig can be pressurized.

The facility basically consists of a liquid pump, two liquid ring gas compressors operating in parallel, a heat exchanger for removing the heat of compression, small liquid pump for recirculating the cooling liquid to the compressor inlet, main separator tank, and compressor outlet separator tank.

The rig works as follows: the liquid is kept in the main separator and is directed by the liquid pump into the mixer at the base of the riser. The gas is moved into the mixer by the liquid ring compressors. The two phases are combined in the mixer from where the gas/liquid flow begins its development in the 11 meter high riser. The Wire Mesh Sensor is positioned towards the top of the riser. The flow is then directed into the downcomer, which is connected to the main separator where the liquid separated from the gas. The flow rates of the fluids are regulated by valves, and measured by flow meters. The main measurement instrument used was a 32x32 wire mesh sensor. The information about using of wire mesh sensors by other workers and its' working principle is presented later in this chapter. The rig is equipped with pressure transducers, temperature measurement instruments. The electronic instruments are connected to a computer where the data is collected by Labview software. Figure 3.2, 3.3 show some of the important pieces of the rig.

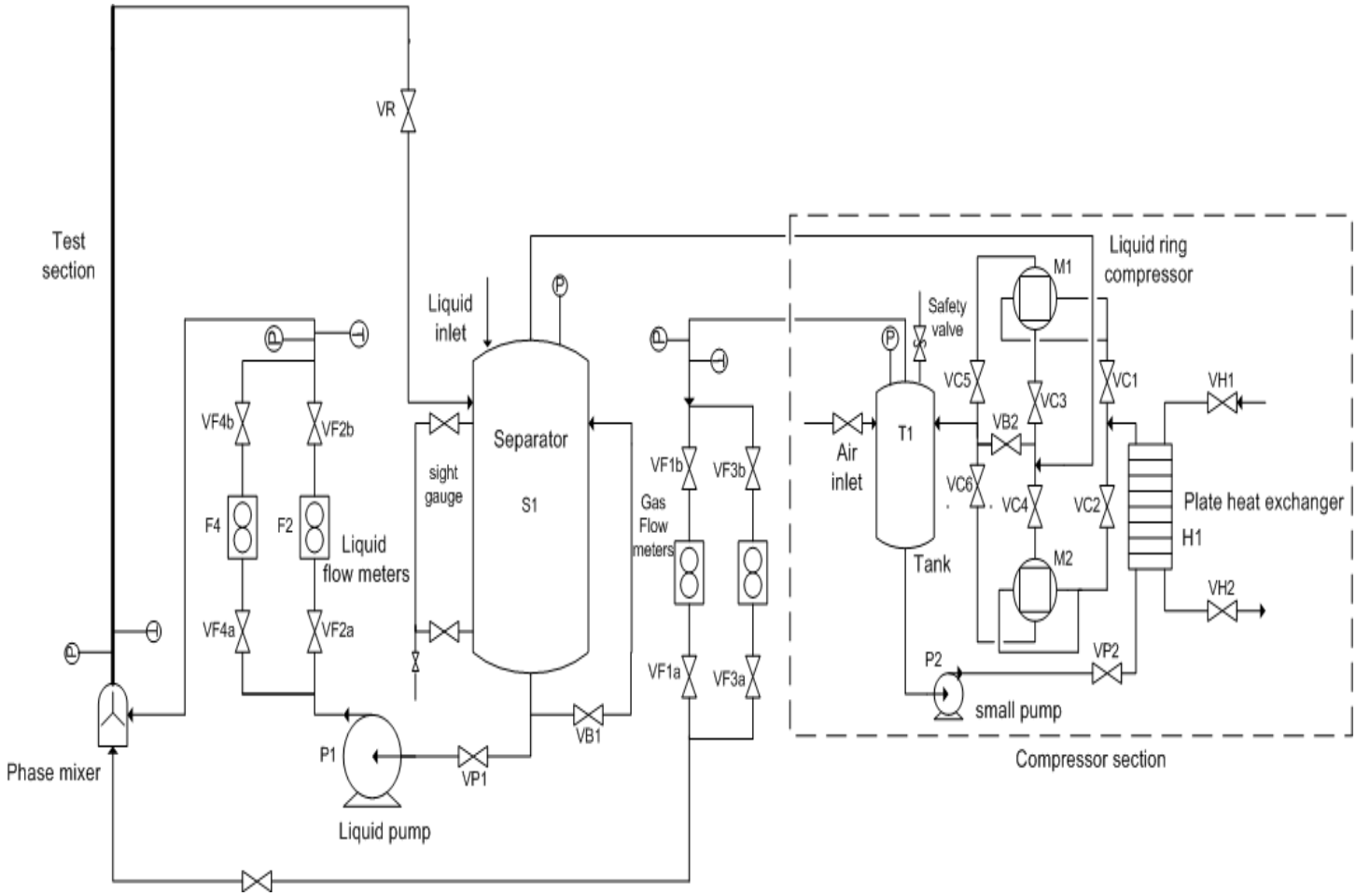

Figure 3.1 The schematic diagram of the experimental facility, (M. Zagana et al 2010)

Figure 3.2 The liquid ring vacuum compressors and the heat exchanger

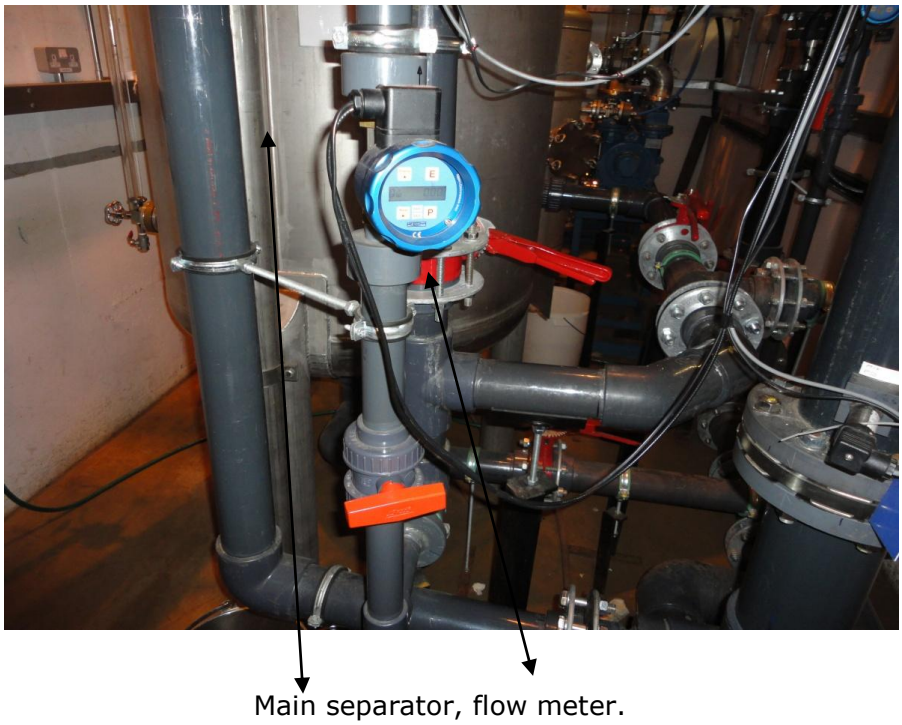

Figure 3.3 Main separator tank, piping, flow meter, valves

3.2 Wire mesh sensor

3.2.1 Introduction

Multiphase flows occur in a variety of processes and equipment including food and drink processing, chemical reactors, drug production, petroleum industry and many others. Multiphase flow often plays a very important role for the safety and productivity of processes in which it occurs. That is why the ability to understand, predict and measure multiphase flow is highly essential. Moreover, reliable experimental data is also needed for the development and validation of computational fluid dynamics (CFD) codes. Several techniques have been used to measure and visualize multiphase flows (Boyer et al 2002). Today there is no a sole measurement technique or sensor for multiphase flow. This comes from the fact that multiphase flow occurs in a wide variety of ways and conditions – dilute and dense particulate systems in process plants, bubbly columns, and pipelines. A vessel can be made of acrylic glass in low pressure and low temperature applications and allow optical observation but can be of thick steel or compound materials in case of high temperature and pressure. Therefore present measurement or visualization methods are more or less appropriate depending on the type of flow, material of the enclosures for spatial and temporal resolution. Presently homographic methods such as electrical resistance or capacitance tomography, gamma ray tomography, or X-ray tomography are considered highly promising as they work noninvasively (Thiele et al 2009). However electrical tomography techniques have serious spatial resolution restrictions, whereas tomography techniques based on ionizing radiation are expensive and often quite slow. Particularly for the study of transient flow phenomena quick sensors with high spatial resolutions are needed. Because of that a sensor called wire-mesh sensor has been widely used by many workers (Abdulkareem et al 2009 (a), Abdulkareem et al 2009 (b), Pietruske and Prasser 2007 and many other). It has a wire electrode mesh in the flow cross section to measure electrical conductivity or permittivity in the crossings of the wire. It should be noticed that often several measurement techniques are used at the same time for comparison reasons (Azzopardi et al 2010, Hunt 2010 et al, Abdulkareem 2009(a), AbdulKareem 2009(b)).

3.2.2 The wire mesh sensor of this thesis

The sensor is sensitive to the electrical conductivity of the fluids. In case of water/air flow, the water is conducting, whilst the gas phase is almost an ideal insulator. The sensor is composed of two grids of parallel wires which are located over the measured cross section, figure 3.4. The wires of both planes cross under 90 degrees.

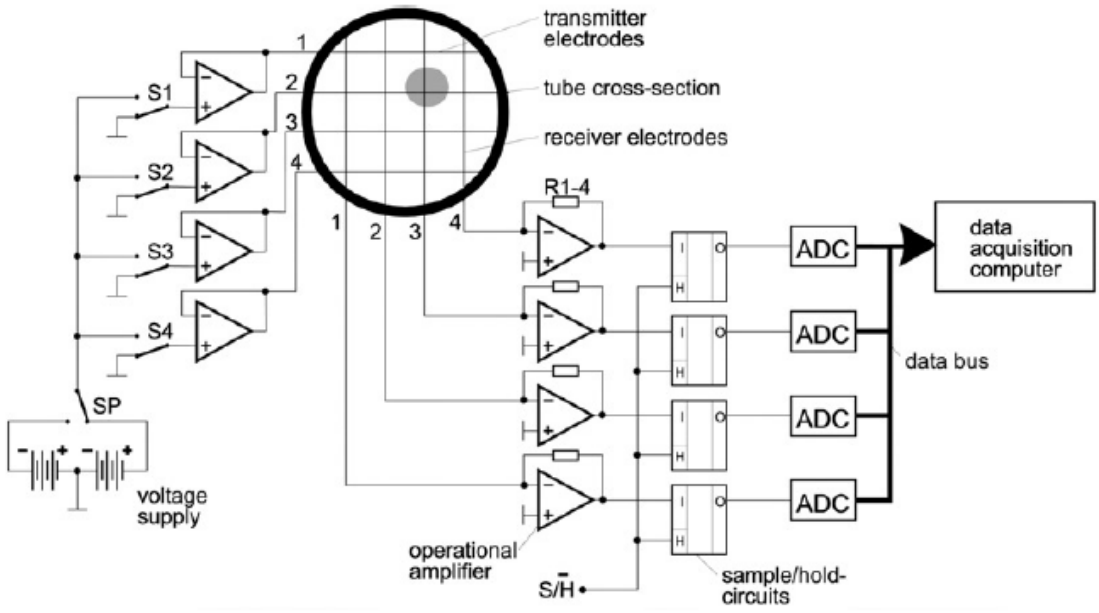

Figure 3.4 Simplified scheme of a wire mesh sensor. (Pietruske and Prasser 2007)

In this work a 32 × 32 wire configuration sensor was employed. The sensor consists of two planes of 32 stainless steel wires of 0.12 mm in diameter, 2 mm axial plane distance. The wires are uniformly distributed over the tube cross section. The spatial resolution of the images produced by the sensor is 3.85 mm. The sensor is installed on an acrylic frame which allows installation on the test section.

An associated electronics measures the local permittivity between the planes in all crossing points by using an excitation voltage to each one of the sensor electrodes at one wire plane during the measurement on parallel the current going towards receiver electrodes at the other wire plane. The non activated transmitter wires are grounded. This step makes sure

that the electrical field distribution is concentrated along the active wire and allows for sampling only a certain area within the tube, so that the measured currents are definitely related to the corresponding crossing point. For the sampling a sinusoidal alternating voltage is used and demodulation technique is employed. After digitalization data directed to a computer where the data is displayed and processed.

The principle of work of the wire mesh sensor is the direct and high speed imaging of the flow based on capacitance sampling of wires crossing points. Image reconstruction is not required, i.e., solving an inverse problem as for the tomography method. The wire mesh divides the flow channel cross section into a number of separated areas where every crossing point presents one area.

The output reading of a wire mesh sensor comes as data matrix V(i,j,k) presenting the voltage measured at each (i, j) crossing point with $i \in$ (1, ..., 0.32) and $j \in$ (1, ..., 0.32) and at a given time step k. These voltage readings are proportional to the corresponding permittivity of two phase mixture ε_m:

$$V = a \cdot \ln(\varepsilon_m) + b. \qquad (3.1)$$

Here a and b are constants that cover the specific parameters of the electronics. Measurements are needed to determine the constant a and b in equation (1), which permits the calculation of mixture permittivity at every crossing point. At first the sensor measures the empty tube, i.e., gas ($\varepsilon_{r,G}$ =1), giving the reference data matrix $V_G(i, j)$ which normally an average of the raw data over a sufficient temporal range to suppress the noise. The procedure is repeated with the whole cross section covered with liquid phase with a permittivity value $\varepsilon_{r,L}$ i.e., full tube which provides another reference data matrix. Eventually on the basis of the equation (1) for the two conditions described the measured mixture permittivity is calculated by:

$$\varepsilon_m(i,j,k) = \exp\left(\frac{V(i,j,k) - V^G(i,j)}{V_{L(i,j)} - V_{G(i,j)}} \ln(\varepsilon_r, \mathrm{L})\right) \quad (3.2)$$

There are different ways of describing the effective permittivity of a two substance mixture based on different assumptions of how the phases are geometrically distributed in the flow. The most generally used for gas/liquid flows is the parallel model which enunciates that the effective permittivity linearly depends on the phase fraction. The void fraction is gained from the measured permittivity ε_m according to:

$$\alpha(i,j,k) = \frac{\varepsilon r,L - \varepsilon m(i,j,k)}{\varepsilon r,L - \varepsilon r,G} \quad (3.3)$$

Where $\varepsilon_{r,L}$ is the liquid permittivity and $\varepsilon_{r,G} = 1$ is the gas permittivity.

To analyze the void fraction data $\alpha(i,j,k)$, which is a 3D matrix, different levels of complexity may be employed. For example image sequences of the flow and cross section images from the pipeline can be obtained. Three-dimensional contour pictures of gas/liquid interface can be produced, illustrating for example the shape of bubbles. Quantitative insights of the flow are gained by averaging the measured void fraction in space and or time, giving a time series of void fraction or mean void fraction over the entire measurement. A unique characteristic of wire mesh sensor owe to its high spatial and temporal resolution is that single bubbles can be measured (Azzopardi et al 2010).

3.2.3 The shortlist of the wire mesh characteristics

The wire mesh sensor used in this work has the following characteristics Sharaf (2011):

32 transmit and 32 receive wires. Therefore spatial resolution 3.85mm

- Temporal resolution 1000 frames per second (can work up to 10,000Hz)
- Two planes of wire mesh; separation of two meshes 2 mm
- Size of wires 0.12 mm in diameter (stainless steel)
- Maximum design pressure 30 bar (Max. working pressure 20 bar)
- Maximum temperature 80°C
- Relative permittivity 1 (air) to 80 (H2O). Silicone Oil ~2.7

Chapter 4 Experimental data and analysis

A total of 81 runs were performed measuring void fraction, pressure, flow rates and temperature for a range of liquid superficial velocities from 0.0165 m/s to 0.51 m/s and the gas superficial velocity from 3 m/s to 16.4 m/s. The experiments were done at three sets of pressure 0, 1, 2. Several methods of analysis which have been used in this work to obtain the knowledge of flow behavior are described in this chapter.

4.1 Uncertainty limits

This subchapter deals with uncertainties of the measurements. There have been three sets of measurements at each pressure 0, 1, 2.

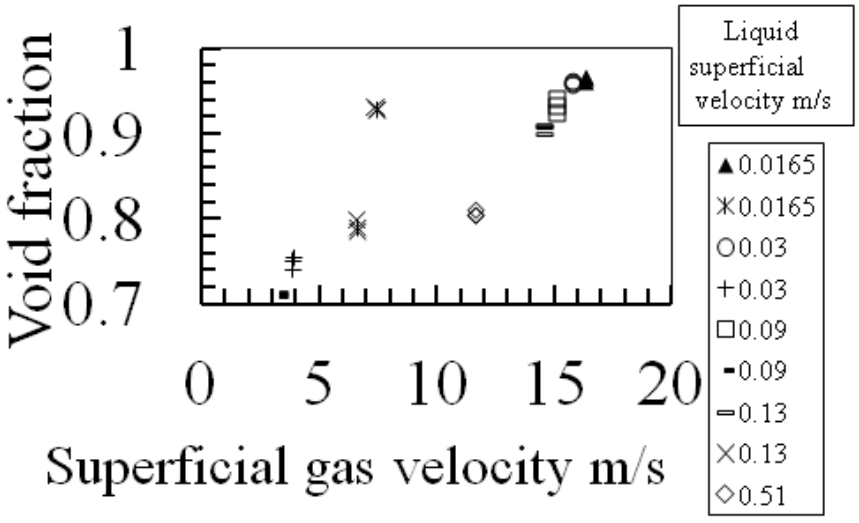

Figure 4.1 Void fraction measurements at 2 bar.

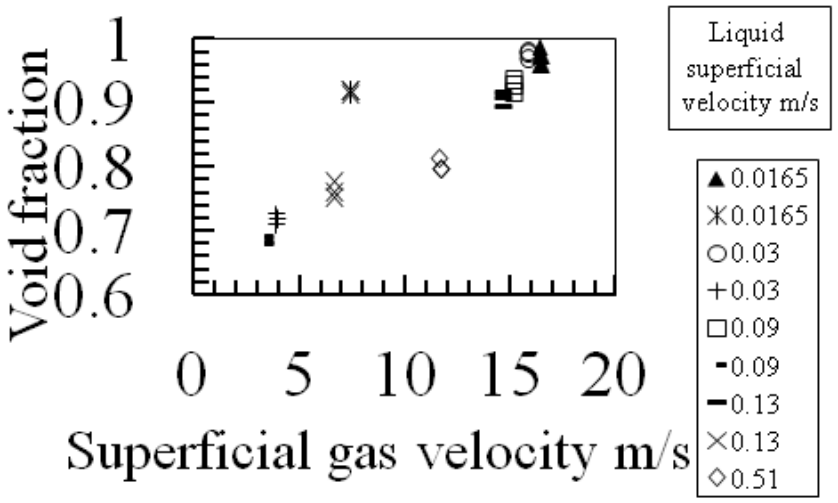

Figure 4.2 Void fraction measurements at 1 bar

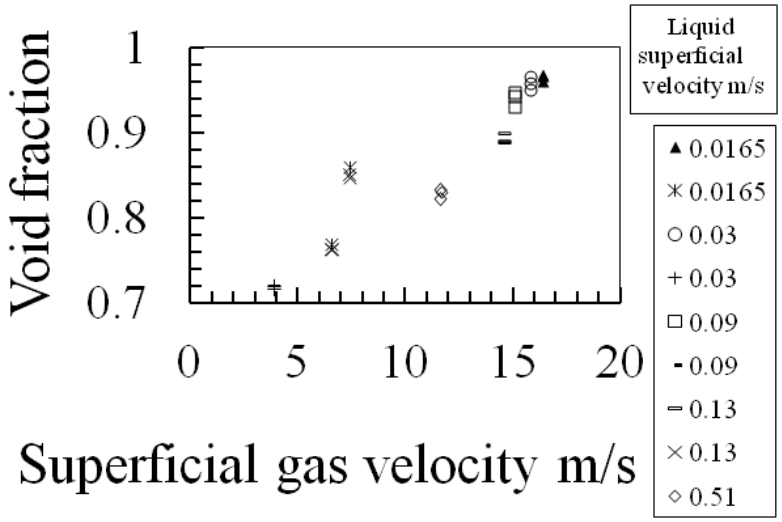

Figure 4.3 Measurements of void fraction at 0 bar.

From the figures 4.1, 4.2, 4.3 it is clear that the difference in the void fraction at each point is very small and does not exceed 1%, the results are nearly the same. This says that the results are reliable. For the analysis the average of the measurements was used.

According to Sharaf (2011) the uncertainty of the wire mesh itself is around 10%. Together with the average uncertainty it gives around 11%. Figure 4.4 represents the error bars of 11% of the void fraction for the runs at 2 bar pressure.

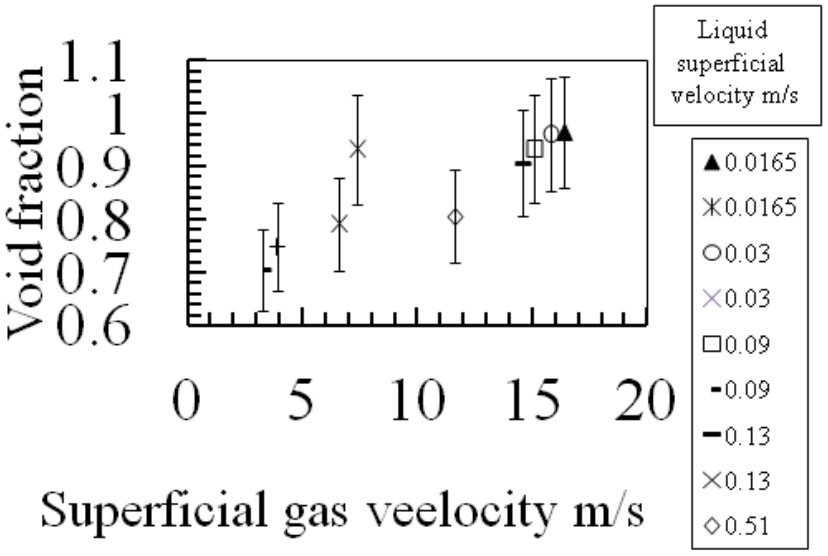

Figure 4.4 Void fraction measurements of the runs at 2 bar with error bars.

4.2 Void fraction

The time average void fraction versus gas superficial velocity at different liquid superficial velocity at 0, 1, 2 bar.

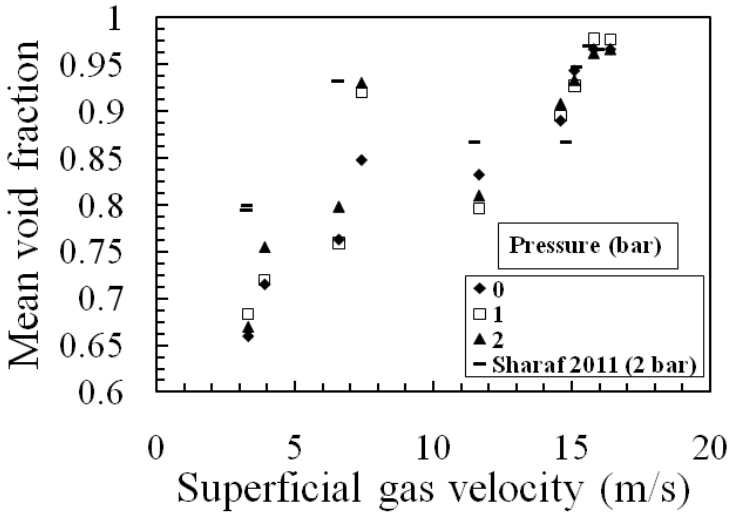

Figure 4.5 Mean void fraction is plotted against gas superficial velocity at different pressure

The graph illustrates that void fraction tends to increase with pressure. As the gas velocity goes up the difference in void fraction for each pressure becomes less, and at higher

gas velocity void fraction of higher pressure runs is equal or even less than void fraction of lower pressure runs. Comparison with Sharaf 2011 results shows the same trend with runs of 2 bars.

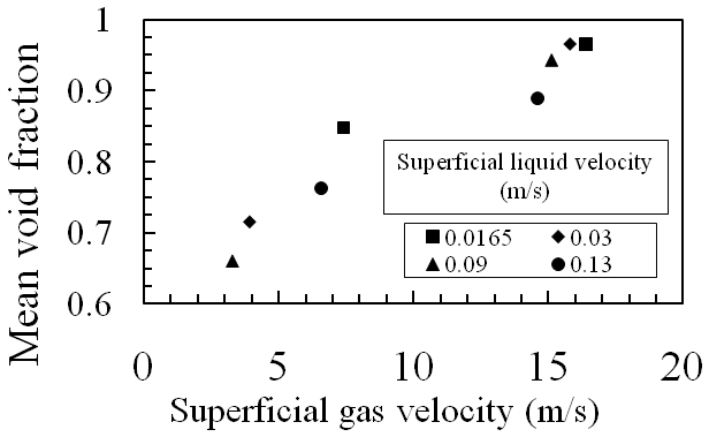

Figure 4.6 Mean void fraction variation with U_{gs} at 0 bar

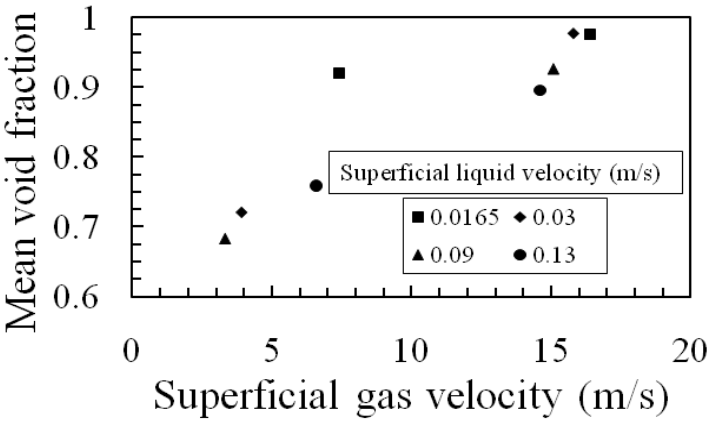

Figure 4.7 Mean void fraction variation with U_{gs} at 1 bar

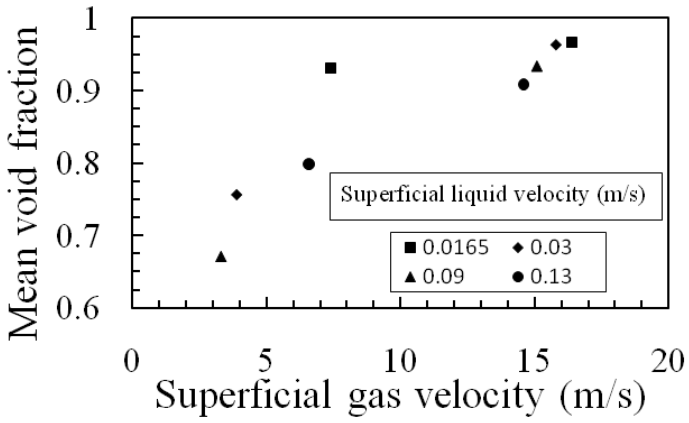

Figure 4.8 Mean void fraction variation with U_{gs} at 2 bar

From the figures 4.6, 4.7, 4.8 it is clear that void fraction increases with increase in superficial gas velocity and goes down with increase in liquid superficial velocity. The same trend has been observed by AbdulKareem et al 2009(b) in 67 mm, Kaji (2008) in 19 mm and 70 mm pipes. The void fraction of 0.0165 m/s of liquid superficial velocity is very high for both 7.4 m/s and 16.4 m/s of gas superficial velocity, it may be because at this flowrates there is a very small amount of liquid in the riser.

4.3 Film thickness

Film thickness is calculated: $F = \left(\frac{D}{2}\right) \times (1 - \varepsilon^{0.5})$

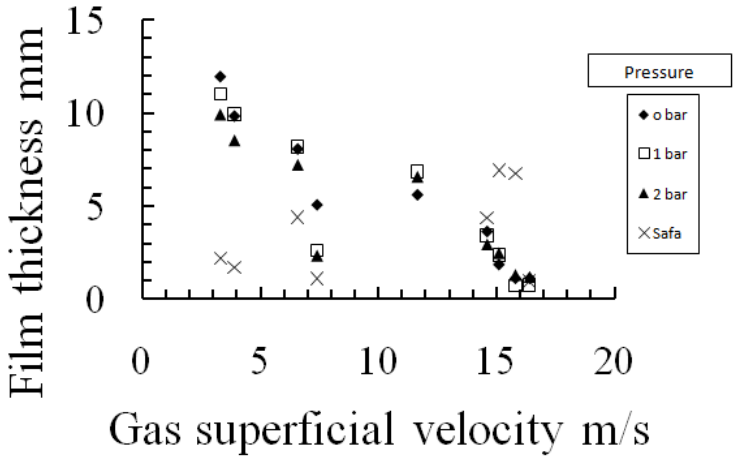

Figure 4.9 The effect of gas superficial velocity on film thickness.

Figure 4.9 demonstrates the effect of gas superficial velocity on film thickness. It can be seen that with increase in gas superficial velocity film thickness decreasing. the same trend is observed by Abdulkareem 2009(b) for liquid film around Taylor bubbles. It is also evident that film thickness tends to decrease with increase in pressure at lower gas superficial velocities, but at higher gas superficial velocities the film thickness is nearly the same at the three pressures.

4.4 Visual images

Visual images were obtained using WMS viewer and display software.

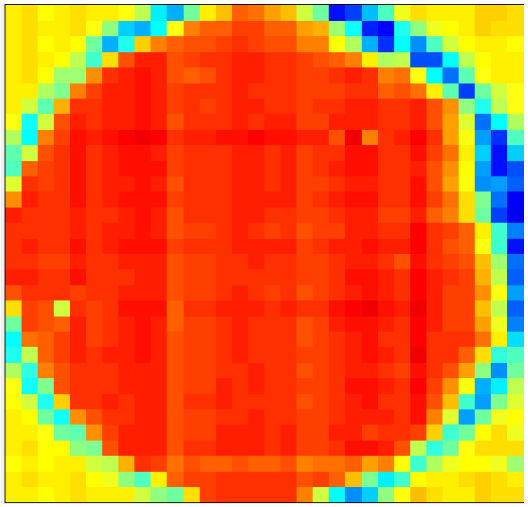

Figure 4.10 Image from WMS viewer software. Superficial liquid velocity 0.0165 m/s, superficial gas velocity 16.4 m/s, 2 bar

Figure 4.10 shows a typical image from WMS viewer, here the red color represents gas and the blue is liquid. In this case it is clearly annular flow and PDF graph in section 4.4 confirms it.

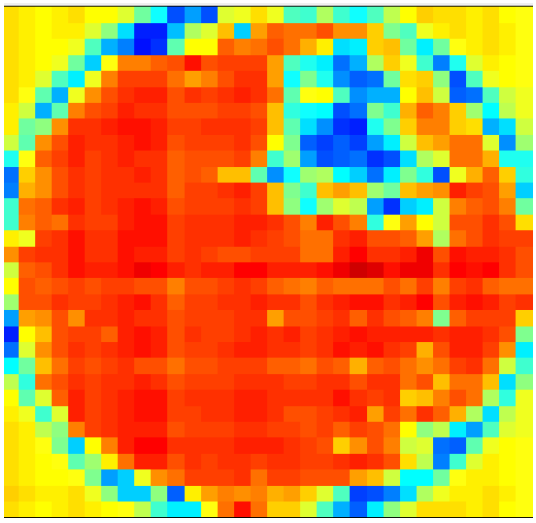

Figure 4.11 Image from WMS viewer software. Superficial liquid velocity 0.0165 m/s, superficial gas velocity 7.4 m/s, 2 bar

Figure 4.11 shows an image of the same superficial liquid velocity as figure 4.9 but for the lower superficial gas velocity. It can be easily seen that the void fraction in this case is less than in case of former flow.

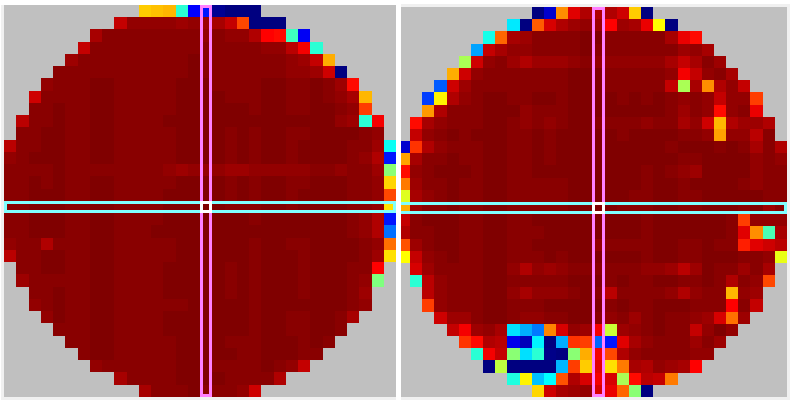

a b

Figure 4.12 Images from WMS display

Figure 4.12 a shows a frontal view of a run with liquid superficial velocity of 0.0165 m/s and superficial gas velocity of 16.4 m/s respectively. Picture b shows a frontal view of a run with superficial liquid velocity of 0.0165 m/s and superficial gas velocity of 7.4 m/s. The red colour represents gas and the blue liquid. Both images are for 2 bar pressure. In picture a it

is clear that nearly the whole pipe is filled with the gas and liquid is on the walls of the pipe - the flow pattern is annular flow, whilst in picture b liquid occupies more space and some of the liquid appears in the core of the pipe, the flow patterns tends to become churn flow.

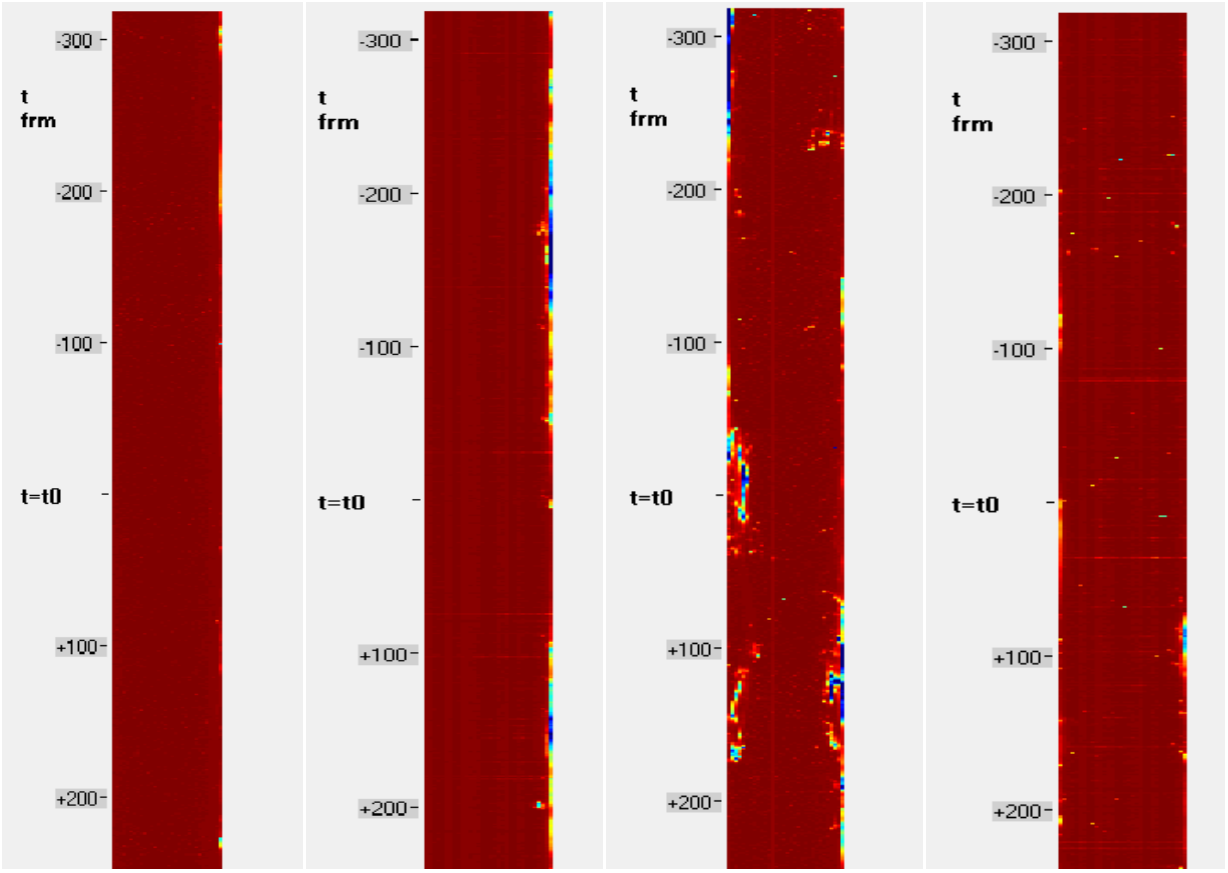

a b c d

Figure 4.13 Image from WMS display

In the figure 4.13 the conditions and the flow patterns are the same with the figure 4.12 a and b but the views are different. Pictures a and b show vertical and horizontal views of a run with liquid superficial velocity of 0.0165 m/s and superficial gas velocity of16.4 m/s respectively (annular flow). Pictures c and d show vertical and horizontal views of a run with superficial liquid velocity 0.0165 m/s and superficial gas velocity 7.4 m/s (becoming churn flow). All the images are for 2 bar pressure. The red colour represents gas and the blue colour liquid

From figure 4.11, 4.12, 4.13 it is evident that amount of water in the middle of the pipe increases with the decrease in superficial gas velocity.

4.5 Probability Density Function

The Probability Density Functions are the means for flow pattern identification. The work of Costigan and Whalley (1997) identified six flow patterns which were discrete bubbles, spherical cap bubbles, stable slug, unstable slug, churn and annular. According to these patterns in the present study only annular and churn flows occurred. For each liquid superficial velocity two runs were done at high and low gas superficial velocity.

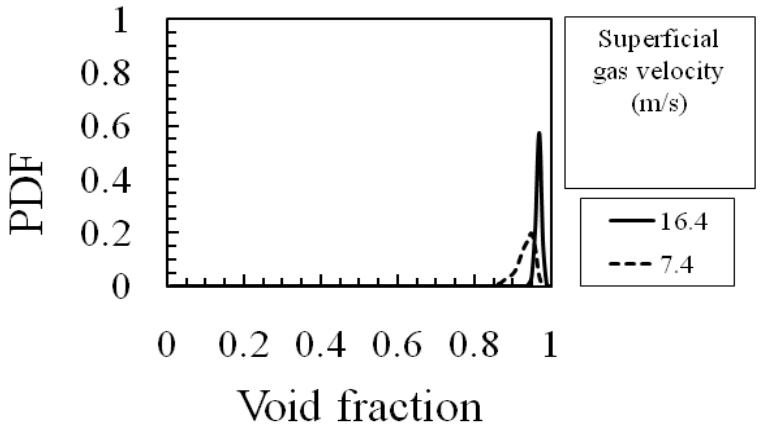

Figure 4.14 Liquid superficial velocity 0.0165 m/s, 2 bar

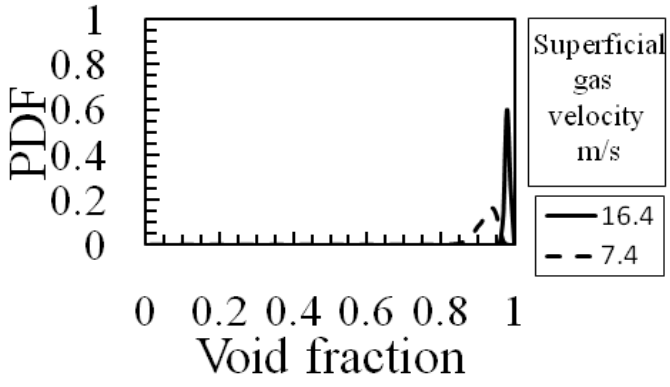

Figure 4.15 Liquid superficial velocity 0.0165 m/s, 1 bar

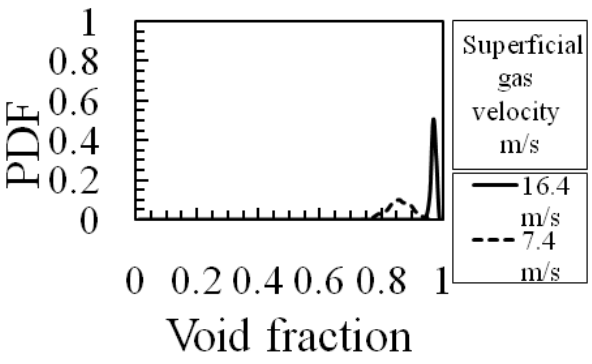

Figure 4.16 Liquid superficial velocity 0.0165 m/s, 0 bar

The figures 4.14, 4.15, 4.16 show that for 16.4 m/s gas superficial velocity there is always annular flow and for pressures of 1 bar and 2 bar the PDFs are almost the same. For 0 bar the value of PDF is slightly less. For 7.4 m/s gas superficial velocity the PDFs of the three pressures are fairly different. It is evident that with the decrease in pressure the value of PDF and void fraction is decreasing. For the other experimental runs the trend is similar.

Chapter 4.5 Frequency

Dominant frequencies from the Wire mesh sensor versus gas superficial velocities were obtained. The frequencies of periodical structures were determined. This was gained by using the methodology of power spectrum density (PSD) technique. According to Maalen (1999) the first part of the curve in figure 4.8 is noise and the real frequency is the next peak.

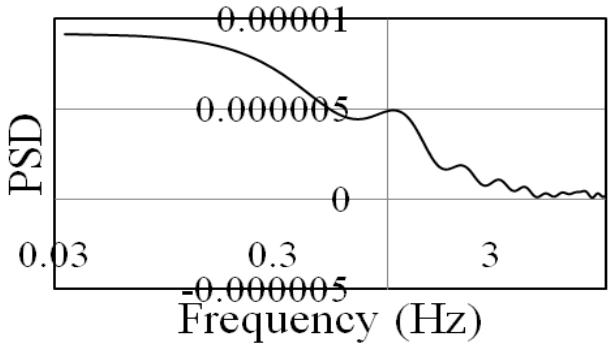

Figure 4.17 Frequency at 0 bar liquid superficial velocity 0.0165 m/s, gas superficial velocity 16.4 m/s.

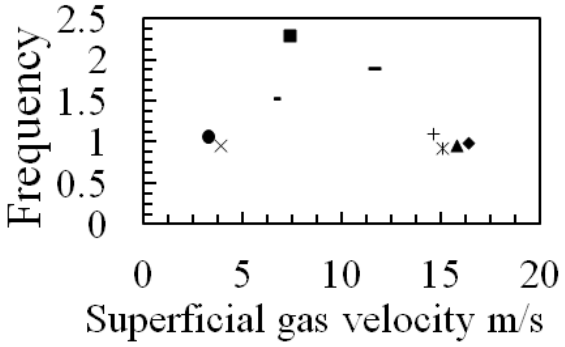

Figure 4.18 Frequency versus gas superficial velocity at 0 bar

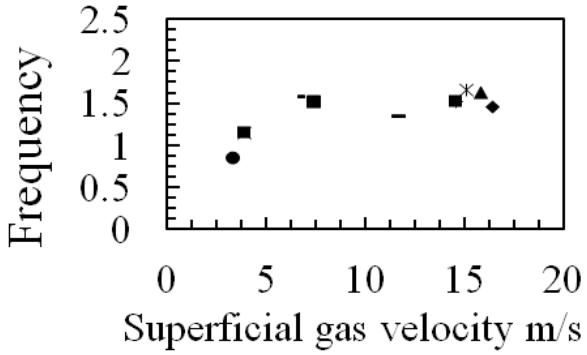

Figure 4.19 Frequency versus gas superficial velocity at 1 bar

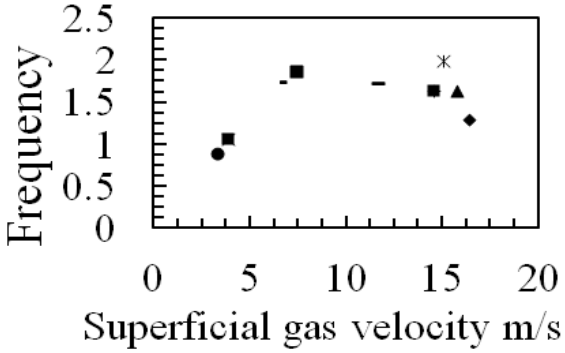

Figure 4.20 Frequency versus gas superficial velocity at 2 bar

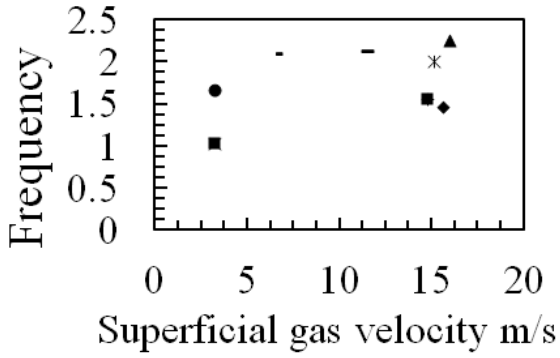

Figure 4.21 Frequency versus gas superficial velocity at 2 bar Sharaf (2011)

The graphs 4.18, 4.19, 4.20, 4.21 show approximately the same trend. At the lower gas superficial velocity the frequency increases, then it starts to decline. It increases again at higher velocity and then show a decrease again.

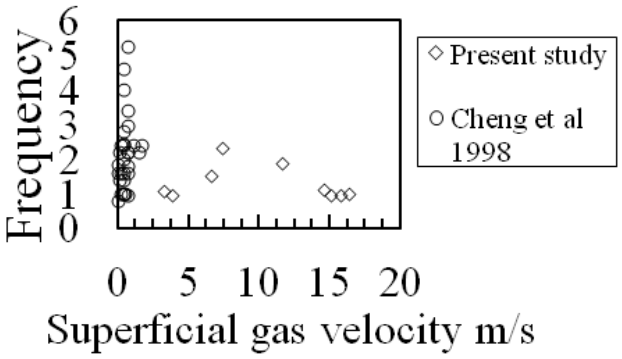

Figure 4.22 Comparison of frequency of the present study with that of Cheng et al 1998

The frequency of the present study was compared with that of Cheng et al (1998) where the measurements of bubbly flow were done in a pipe of 150 mm diameter (figure 4.18). The huge difference is clear, Cheng et al were working at significantly lower gas superficial velocities and with bubbly flow.

4.6 Comparison of void fraction results with prediction models

Comparison of the void fraction of the present data with prediction methods of Beggs and Brill (1973), Chisholm (1983), CISE (Azzopardi (2006)).

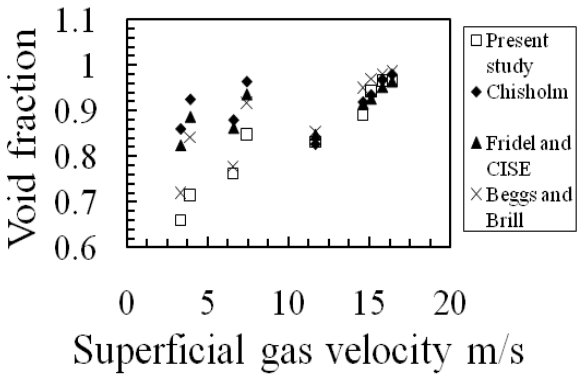

Figure 4.23 Comparison of the present study void fraction results with Chisholm, CISE, Beggs and Brill predictions at 0 bar

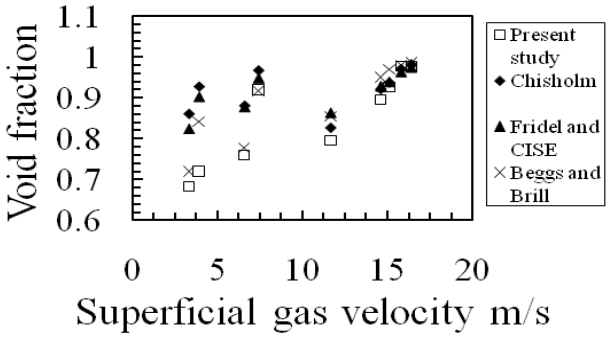

Figure 4.24 Comparison of the present study void fraction results with Chisholm, CISE, Beggs and Brill predictions at 1 bar

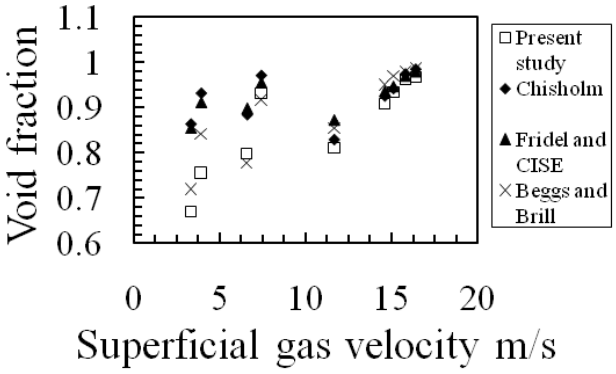

Figure 4.25 Comparison of the present study void fraction results with Chisholm, CISE, Beggs and Brill predictions at 2 bar

Figures 4.23, 4.24, 4.25 show comparison of the present void fraction data with predictions of Chisholm, CISE and Beggs and Brill. It is clear that the data from the four sources coincides at the higher gas superficial velocities at all pressure sets, Beggs and Brill prediction show slightly higher void fraction. When it comes to the lower gas superficial velocities the situations is different, particularly at the first three runs. The models of Chisholm and CISE demonstrate nearly equal results and void fraction predicted by Chisholm is slightly higher at all the pressure sets. The prediction by Beggs and Brill demonstrates the closest values to the void fraction of the present study particularly at 0 and 1 bar. The difference in void fraction may be explained by the fact that in the present study the diameter of the pipe is much larger than in the three prediction methods. It can be concluded, that for higher superficial gas velocities for annular flow in particular Beggs and Brill, Chisholm and CISE predictions are correct, while for lower superficial gas velocities they do not demonstrate right predictions. The prediction by Beggs and Brill, however, can be considered as more or less reliable for the lower superficial gas velocities.

Chapter 5 Conclusions and further work

This chapter denotes the conclusions made in the study and the further work which is encouraged to be done to further explore the effect of the pressure on multiphase flow in vertical pipes.

5.1 Conclusion

In this work the effect of pressure on gas/liquid flow in large diameter vertical riser was investigated. Three series of experiments at 0, 1, 2 bar were carried out to achieve this.

In total 81 experimental runs were performed measuring mean void fraction. For this a wire mesh sensor was employed. Data was analyzed in several ways, for flow pattern identification PDF graphs were plotted, it was found that in the present study annular and churn flows occurred. Dominant frequencies for each run were obtained and plotted against gas superficial velocity using PSD technique. Frequency was also compared with that of Cheng et al 1998. Mean void fraction and film thickness of the runs done at two bar was compared with that of Sharaf (2011), it was found that the results from the two studies are not the same but quite close to each other. The void fraction obtained was also compared

against predictions by Chisholm, Beggs and Brill and CISE. It was found that for higher superficial gas velocities all the methods show reliable predictions while for lower superficial gas velocities there is significant difference between experimental data of this study and the predictions. However Beggs and Brill prediction was more or less close to the experimental results at both low and high superficial gas velocities. The difference may be explained by the fact that the predictions were developed using experimental data from smaller diameter pipes.

The information obtained in this study constitutes a valuable data base for further reaserch in this field.

5.2 Future work

In order to investigate the effect of pressure on multiphase flow more thoroughly, the following suggestions are encouraged to perform in the future.

- Make the step of pressure change less: 0, 0.5, 1, etc.
- Try pipes of different diameter
- Investigate different fluids
- Investigate influence of pipe inclination

Nomenclature

Symbol	Alternative symbol	Description	Units	Alternative unit
C		Wallis parameter		
D	d	Diameter	mm	m
F_{wL}		Frictional pressure drop	bar	
f		Frequency	Hz	
f_{bc}		Bubble collision frequency		
f_o		Total liquid flow	m^3/day	

		rate		
L		Pipe length	m	mm
P		Pressure	bar	Mpa
Q_g		Gas flow rate	kg/min	m^3/s
Q_w		Liquid flow rate	kg/min	m^3/s
r_B		Bubble radius	mm	
T		Temperature	C	
U_{gs}		Superficial gas velocity	m/s	
U_g^*		Dimensionless gas velocity		
U_{gm}		Superficial liquid velocity	m/s	
U_g^*		Dimensionless liquid velocity		
We		Weber number		
We_{crit}		Critical Weber number		
Z		Axial distance	mm	

Greek symbols

Symbol	Alternative symbol	Description	Units	Alternative unit
ρ		Density	kg/m^3	
ε		Void fraction		
ν^2		Spatial average value		
σ		Surface tension	kg/s^2	

η		Viscosity (dynamic)	Kg/ms	
τ_w		Wall shear stress	N/m^2	

References

Abdulkareem L.A, V. Hernandez-Perez, B.J. Azzopardi, S. Sharaf, S. Thiele, M. Da Silva. (2009(a)) "Comparison of different tools to study gas-liquid flow." ExHFT-7, Krakow, Poland

AbdulKareem, L. A, Azzopardi B. J., Thiele S., Hunt, A., Marco J. Da Silva. (2009(b)), "Integration of gas/liquid flow in a vertical using two tomographic techniques." Proceedings of the ASME 28th International Conference on Ocean, Offshore and Arctic Engineering OMAE Honolulu, Hawaii

Azzopardi B. J., Abdulkareem L., Zhao D., Thiele S., Da Silva M. J., Beyer M, A. Hunt, (2010). "Comparison between Electrical Capacitance Tomography and Wire Mesh Sensor Output for Air/Silicone Oil Flow in a Vertical Pipe." Ind. Eng. Chem. Res., 49, 8805–8811

Azzopardi, B.J. and Hills, J. (2001) Published in Bertola, V. (2003) "Modeling and Experientation in two phase flow." CISM courses and lectures No 450, International Centre for Mechanical Science, ISBN 3-211-20757-0, Springer – Verlag Wien New York.

Baily, R.V., et al. (1956). "Transport of gases through liquid-gas mixture." Paper presented at the AIChE New Orleans meeting.

Beggs, H.D., and Brill, J.P. (1973) "A study of two-phase flow in inclined pipes." Journal of Petroleum Technology,25:607-617.

Boyer C, A. M. Duquenne, and G. Wild, (2002) "Measuring techniques in gas-liquid and gas-liquid-solid reactors," Chem. Eng. Sci., vol. 57, no. 16, pp. 3185–3215.

Brauner, N., and Barnea, D. (1986) "Slug/churn transition in upward gas-liquid flow." Chemical Engineering Science 40:159-163.

Cheng H, J. H. Hills and B. J. Azzorpardi (1998). "A study of the bubble-to-slug transition in vertical gas/liquid flow in columns of different diameter." International Journal of Multiphase Flow, Volume 24, Issue 3, Pages 431-452

Chisholm, D (1983) "Two-phase flow in pipelines and heat exchangers." London and New York, The Institution of Chemical Engineers.

Coney, M.W.E. (1974) "The analysis of a mechanism of liquid replenishment and draining in horizontal two-phase flow." International Journal of Multiphase Flow 1:647-670.

Costigan, G., Whalley, P.B., (1997). "Slug flow regime identification from dynamic void fraction measurements in vertical air–water flows." Int. J. Multiphase Flow 23, 263–282.

Da Silva, M. J., Thiele, S., Abdulkareem, L., Azzopardi, B. J., Hampel, U. 2009 "High-resolution gas-oil two-phase flow visualization with acapacitance wire-mesh sensor." Flow Meas. Instrum., DOI: 10.1016.

Duan X.Y., S.C.P.Cheung, G.H.Yeoh, J.Y.Tu, E.Krepper, D.Lucas. (2011) "Gas–liquid flows in medium and large vertical pipes." Chemical Engineering Science 66 872–883.

Govan, A. H., Hewitt, G. F., Richter, H. J., and Scott, A. (1991) "Flooding and churn flow in vertical pipes." International Journal of Multiphase Flow 17:27-44.

Hewitt, G.F., and Roberts, D.N. (1969) "Studies of two-phase patterns by simultaneous x-ray and flash photography." UKAEA Report AERE M2159.

Hibiki, T., Ishii, M., (2003) "One-dimensional drift-flux model for two-phase flow in a large diameter pipe." Int. J. Heat Mass Transf. 46 (10), 1773–1790

Hills, J.H., (1976) "The operation of a bubble column at high throughputs." I. Gas Holdup Measurements. Chem. Eng. J. 12, 88–99.

Hunt A., L.A. Abdulkareem and B.J. Azzopardi (2010) "Measurement of Dynamic Properties of Vertical Gas-Liquid Flow." 7th International Conference on Multiphase Flow ICMF, Tampa, FL USA, May 30-June 4.

Hinze, J.O. (1955) "Fundamentals of the hydrodynamic mechanism of splitting of dispersion processes." American Institute of Chemical Engineers Journal 1:289-295.

Jayanti, S, and Hewitt, G.F. (1992) "Prediction of the slug-to-churn transition in vertical two-phase flow." International Journal of Multiphase Flow 18:847-860.

Jin, N.D., Zhao, X., Wang, J., Jia, X.H., Chen, W.P., (2008) "Design and geometry optimization of a conductivity probe with a vertical multiple electrode array for measuring volume fraction and axial velocity of two phase flow." Meas. Sci. Technol. 19, 045403.

Kaji R. (2008) PhD thesis. "Characteristics of two-phase flow structures and transitions in vertical upflow." The University of Nottingham.

Lempel, A., Ziv, J., (1976) "On the complexity of finite sequences" IEEE Transactions on Information Theory (IT) 22 (1), 75–81.

Lucas, D., Krepper, E., Prasser, H.M., (2005) "Development of co-current air-water flow in a vertical pipe." International Journal of Multiphase Flow 31, 1304–1328.

Maalen H.R.E. (1999) "Retrieval of turbulence and turbulence properties from randomly sampled laser-dopper anemometry data with noise." Muiden, Netherlands.

McQuillan, K.W., and Whalley, P.B. (1985) "Flow patterns in vertical two-phase flow." International Journal of Multiphase Flow 11:161-176.

Mi, Y., Ishii, M., Tsoukalas, L.H., (2001) Investigation of vertical slug flow with advanced two-phase flow instrumentation. Nucl. Eng. Des. 204 (1–3), 87–100.

Mishima, K., and Ishii, M. (1984) "Flow regime transition criteria for upward two-phase flow in vertical tubes." International Journal of Heat and Mass Transfer 27:723-736.

Nicklin, D.J., and Davidson, J.F. (1962) "The onset of instability in two-phase slug flow." Institution of Mechanical Engineers Symposium on Two-Phase Flow, London.

Oddie G., H. Shi, L.J. Durlofsky, K. Aziz, B. Pfeffer, J.A. Holmes. (2003) "Experimental study of two and three phase flowsin large diameter inclined pipes." International Journal of Multiphase Flow 29 527–558.

Ohnuki, A., Akimoto, H., (2000) "Experimental study on transition of flow pattern and phase distribution in upward air–water two-phase flow along a large vertical pipe." Int. J. Multiphase Flow 26, 267–286.

Omebere-Iyari N.K., B.J. Azzopardi, D. Lucas, M. Beyer, H-M Prasser. (2008) "The characteristics of gas/liquid flow in large risers at high pressures." International Journal of Multiphase Flow 34 461–476.

N. K. Omebere-Iyari and B. J. Azzopardi, (2007) "Two-Phase Flow Patterns in Large Diameter Vertical Pipes at High Pressures." American Institute of Chemical Engineers AIChE J, 53: 2493–2504.

Petalas, N., Aziz, K., (2000) "A mechanistic model for multiphase flow in pipe." J. Can. Pet. Technol. 39, 43–55.

Pietruske H., Prasser., (2007) "Wire-mesh sensors for high-resolving two-phase flow studies at high pressures and temperatures." Flow Measurement and Instrumentation 18 87–94.

Prasser, H.-M., Bottger, A., Zschau, J., (1998) "A new electrode-mesh tomograph for gas–liquid flows." Flow Measur. Instrument. 9, 111–119.

Prasser, H.-M., Beyer, M., Bottger, A., Carl, H., Lucas, D., Schaffrath, A.,Schutz, P., Weiss, F.P., Zschau, J., (2005(a)). "Influence of the pipe diameter on the structure of the gas–liquid interface in a vertical two phase pipe flow." Nucl. Technol. 152, 3–22.

Prasser, H.-M., Beyer, M., Carl, H., Gregor, S., Lucas, D., Pietruske, H., Schutz, P., Weiss, F.P., (2005(b)) "Evolution of the structure of a gas–liquid two-phase flow in a large vertical pipe." In: Proceedings of the 11th International Topical Meeting on Nuclear Reactor Thermal-Hydraulics, CD-ROM, #399.

Prasser, H.M., Beyer, M., Carl, H., Gregor, S., Lucas, D., Pietruske, H., Schutz, P., Weiss, F.P., (2007). "Evolution of the structure of a gas-liquid two-phase flow in a large vertical pipe." Nuclear Engineering and Design 237, 1848–1861.

Radovcich, N.A., and Moissis, R. (1962) "The transition from two-phase bubble flow to slug flow." MIT Report No. 7-7673-22.

Richter S., Aritomi M., Prasser H. M., Hampel R.. (2002) "Approach towards spatial phase reconstruction in transient bubbly flow using a wire mesh sensor." International journal of heat and mass transfer 45 103-1075.

Sakaguchi, T., Akagawa, K., Hamaguchi, H., Imoto, M., and Ishida, S. (1979) "Flow regime maps for developing steady air-water two-phase flow in horizontal tubes." Memoirs of the Faculty of Engineering of Kobe University 25:191-202.

Sharaf Safa (2011) Private communication.

Sawai, T., Kaji, M., Kasugai, T., Nakashima, H. & Mori, T. (2004) "Gas–liquid interfacial structure and pressure drop characteristics of churn flow." Experimental Thermal and Fluid Science, Vol. 28, 597-606

Sevik, M., and Park, S.H. (1973) "The splitting of drops and bubbles by turbulent fluid flow." Journal of Fluids Engineering 95:53-60.

Schlegel J.P., P. Sawant, S. Paranjape, B. Ozar, T. Hibiki, M. Ishii. (2009) "Void fraction and flow regime in adiabatic upward two-phase flow in large diameter vertical pipes." Nuclear Engineering and Design 239 2864–2874

Taitel, Y., Barnea, D., Dukler, A.E., (1980) "Modelling flow pattern transitions for steady upward gas–liquid flow in vertical tubes." Am. Inst. Chem. Eng. J. 26, 345–354.

Thiele S, Marco Jose Da Silva, Uwe Hampel (2009). "Capacitance Planar Array Sensor for Fast Multiphase Flow Imaging." IEEE sensors journal, volume 9, number 5.

Vijayan, M., Jayanti, S., and Balakrishnan, A.R. (2001) "Effect of tube diameter on flooding." International Journal of Multiphase Flow 27:797-816.

Wallis, G.B. (1961) "Flooding velocities for air and water in vertical tubes." UKAEA Report AEEW R123.

Wang, N.D.Jin , Z.K.Gao, Y.B.Zong, T.Wang. (2010) "Nonlinear dynamical analysis of large diameter vertical upward oil–gas–water three-phase flow pattern characteristics." Chemical Engineering Science 65 5226–523.

Watson, M.J., and Hewitt, G.F. (1998) "Effect of diameter on the flooding initiation mechanism." 3rd International Conference on Multiphase Flow, Lyon, 8-12 June.

Watson, M.J., and Hewitt, G.F. (1999) "Pressure effects on the slug to churn transition." International Journal of Multiphase Flow 25:1225-1241.

Willetts, I.P., Azzopardi, B.J. and Whalley, P.B. (1987), "The effect of gas and liquid properties on annular two-phase flow", 3rd International Conference on Multiphase Flow, The Hague, The Netherlands, 18-20 May (BHRA pub.).

Xiuzhong Shena, Ryota Matsuia, Kaichiro Mishimaa, Hideo Nakamurab. (2010) "Distribution parameter and drift velocity for two-phase flow in a large diameter pipe." Nuclear Engineering and Design 240 3991–4000.

Yan-Bo Zong, Ning-De Jin *, Zhen-Ya Wang, Zhong-Ke Gao, Chun Wang (2010). "Nonlinear dynamic analysis of large diameter inclined oil–water two phase flow pattern." International Journal of Multiphase Flow 36 166–183.

Yoneda, K. Yasuo, A. Okawa (2002) "Flow structure and bubble characteristics of steam-water two-phase flow in a large-diameter pipe." Nucl. Eng. Des. 217, 267–281.

Zabaras, G.J., and Dukler, A.E. (1988) "Countercurrent gas-liquid annular flow including the flooding state." American Institute of Chemical Engineers Journal 34:389-396.

M.Zangana*, G.P.van der Meulen, B.J.Azzopardi. (2010) "The Effect of Gas and Liquid Velocities on Frictional Pressure Drop in Two Phase Flow for Large Diameter Vertical Pipe." 7th International Conference on Multiphase Flow ICMF, Tampa, FL USA, May 30-June 4.

Zhang, J.-P., Grace, J.R., Epstein, N., and Lim, K.S. (1997) "Flow regime identification in gas-liquid flow and three-phase fluidised beds." Chemical Engineering Science 52: 3979-3992.

Zheng, G.B., Jin, N.D., Jia, X.H., Lv, P.J., Liu, X.B., (2008). "Gas–liquid two phase flow measurement method based on combination instrument of turbine flow meter and conductance sensor". Int. J. Multiphase Flow 34, 1031–1047.

Zuber, N., and Findlay, J.A. (1965) "Average volumetric concentration in two-phase flow systems." Journal of Heat Transfer 87:453-468.

Appendix

PDF graphs of the experimental runs

0 bar	1 bar	2 bar	Saraf2 bar
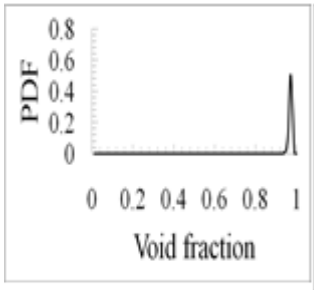	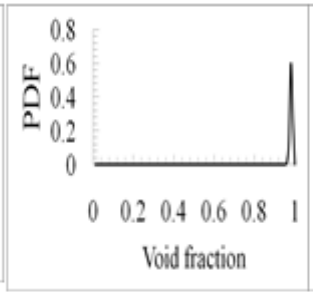	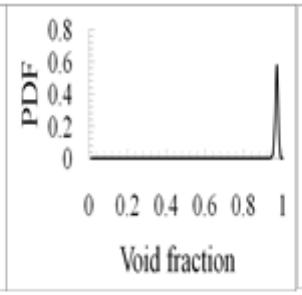	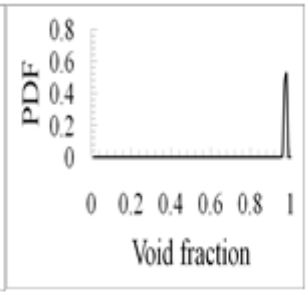
Liquid 0.0165 m/s , Gas 16.4 m/s	Liquid 0.0165 m/s , Gas 16.4 m/s	Liquid 0.0165 m/s , Gas 16.4 m/s	Liquid0.0137 m/s, Gas 15.6 m/s
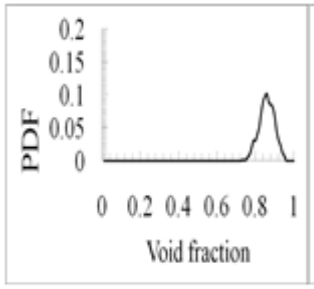	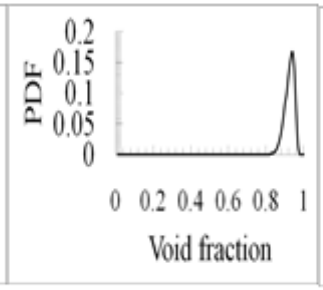	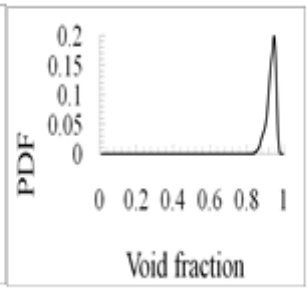	No Data
Liquid 0.0165 m/s, Gas 7.4 m/s	Liquid 0.0165 m/s, Gas 7.4 m/s	Liquid 0.0165 m/s, Gas 7.4 m/s	
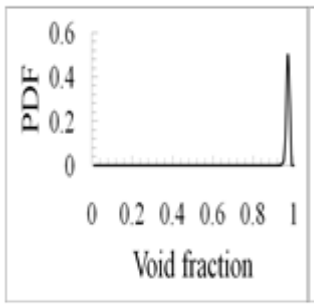	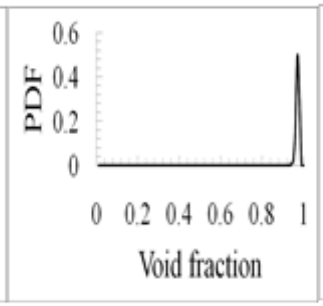	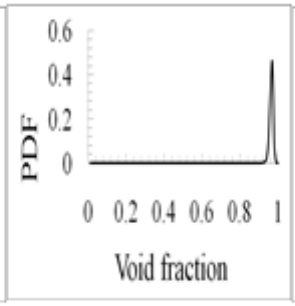	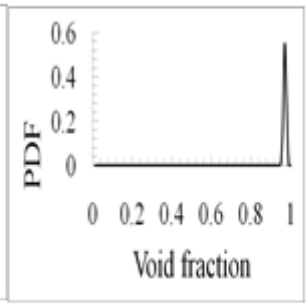
Liquid 0.03 m/s, Gas 15.9 m/s	Liquid 0.03 m/s, Gas 15.9 m/s	Liquid 0.03 m/s, Gas 15.9 m/s	Liquid 0.03 m/s, Gas 15.9 m/s
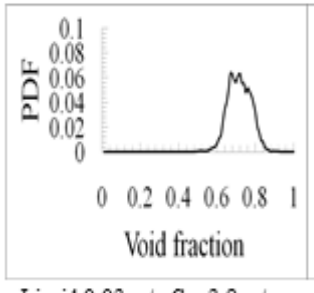	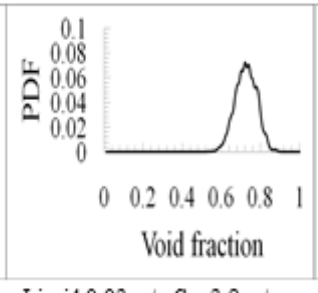	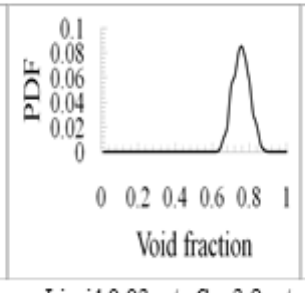	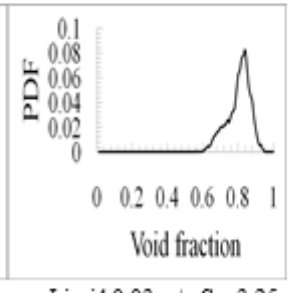
Liquid 0.03 m/s, Gas 3.9 m/s	Liquid 0.03 m/s, Gas 3.9 m/s	Liquid 0.03 m/s, Gas 3.9 m/s	Liquid 0.03 m/s, Gas 3.25 m/s

0 bar	1 bar	2 bar	Safa 2 bar
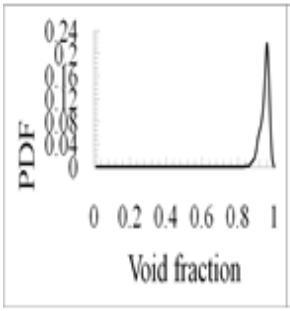	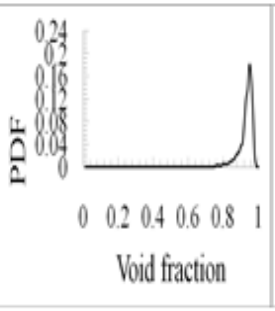	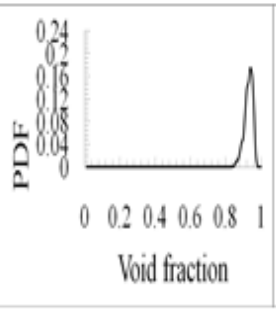	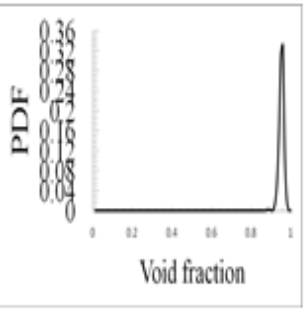
Liquid 0.09 /s, Gas 15.1 m/s	Liquid 0.09 /s, Gas 15.1 m/s	Liquid 0.09 /s, Gas 15.1 m/s	Liquid 0.09 m/s, Gas 15.14 m/s
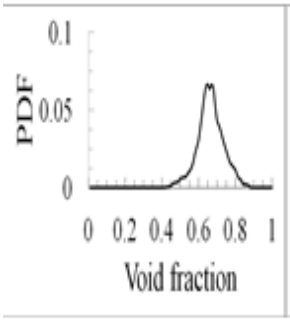	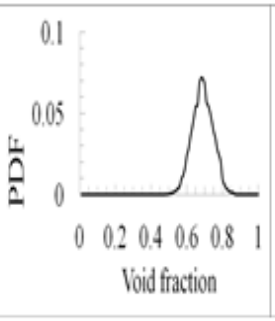	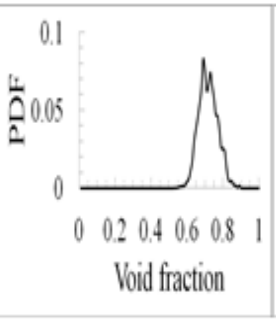	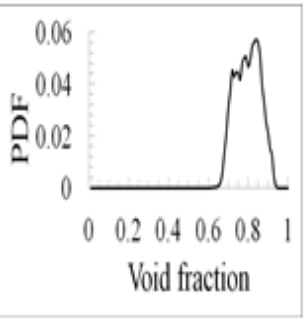
Liquid 0.09 /s, Gas 3.3 m/s	Liquid 0.09 /s, Gas 3.3 m/s	Liquid 0.09 /s, Gas 3.3 m/s	Liquid 0.09 m/s, Gas 3.25 m/s
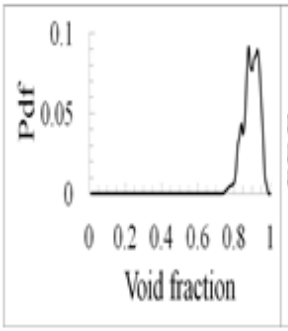	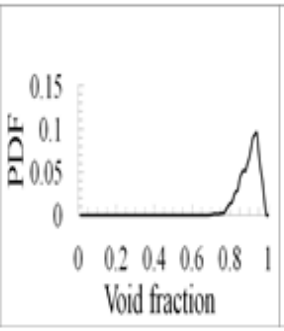	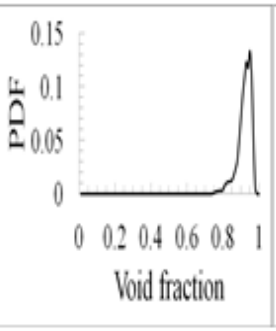	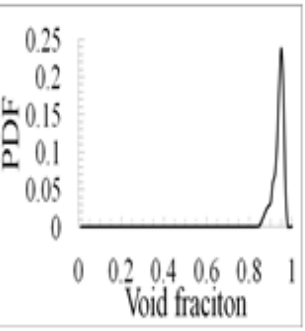
Liquid 0.13 /s, Gas 14.6 m/s	Liquid 0.13 /s, Gas 14.6 m/s	Liquid 0.13 /s, Gas 14.6 m/s	Liquid 0.125 m/s , Gas 14.6 m/s